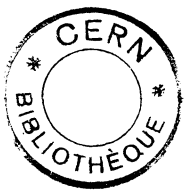

EUROPEAN ORGANIZATION FOR NUCLEAR RESEARCH

EP Internal Report 83-07
8 June 1983

A STUDY OF ^{163}Ho Neutrino Mass Experiments

R.J. Ellis

CERN, Geneva, Switzerland

GENEVA
1983

EUROPEAN ORGANIZATION FOR NUCLEAR RESEARCH

A Study of ^{163}Ho Neutrino Mass Experiments

R.J.Ellis

Abstract: Nine different experiments have been simulated. It appears feasible to put a limit of 100 eV on the neutrino mass and to determine to Q-value to a few volts. It is suggested that the definitive neutrino mass experiment with holmium-163 will use electrons and not photons. It is of great interest to start such an experiment as soon as possible.

0.1. Introduction

Nine different experimental methods for measuring the neutrino mass using ^{163}Ho have been simulated. These divide into three categories:

1. Calorimeter experiments.
2. Internal Bremsstrahlung Electron Capture (IBEC) experiments.
3. And combined calorimeter and IBEC experiments.

Apparatus I in figure 1 is that required for a calorimeter experiment. The Aarhus group has already successfully implanted ^{163}Ho into a solid state detector. Such a detector can measure the relative intensities of the electron capture lines. These are given by:

$$\lambda_{ic} = \frac{g^2}{4\pi^2}\left(M_F^2 + M_{GT}^2\right) n_i \beta_i^2 B_i (Q-E_i)\sqrt{(Q-E_i)^2-m_\nu^2} \qquad (1)$$

where Q=2580±100 eV for ^{163}Ho.

One can define two ratios:

$$R_1 = \frac{\lambda_{M_I}}{\lambda_{N_I}} \qquad (2)$$

$$R_2 = \frac{\lambda_{M_2}}{\lambda_{N_I}} \qquad (3)$$

which are dependent on the atomic terms and phase space term in equation (1) but not the nuclear terms. The atomic terms may be determined by ^{161}Ho in a similar calorimeter experiment. (See apparatus II in figure 1.) A 25.65 keV γ-ray is triggered on by a second detector to ensure that the reaction in the calorimeter is ^{161}Ho(7/2-) → ^{161}Dy(5/2-). (The nuclear matrix element is then almost identical to that for electron capture in ^{163}Ho.) The Q-value for ^{161}Ho is 850 keV and so phase space does not depend significantly on the neutrino mass. Assuming that the atomic terms are known, we can calculate the variation of R_1 and R_2 with the neutrino mass for various Q-values. This is shown in figure 2. It can be seen that the dependence on the mass is smaller than the dependence on the Q-value. Furthermore the statistical error in R_2 is about three times that for R_1 since the M_2 line has an intensity about one tenth that of the M_1 line. So this method might be improved if the Q-value was known more precisely from some independent source. Table I shows an estimate of the precision required. (Here δR^0_{NM} is the error in the atomic part from the ^{161} Ho experiment.) The relevant electron capture lines are shown in table II.

The IBEC spectrum experiments considered are those proposed by De Rujulla [1] and currently being considered by the group. In deciding which is the best IBEC experiment there are several options to consider:

1. One can trigger on a 3p or a 4p spectrum (see figure 4).
2. One can use a solid state detector (resolution independent of photon energy) or a gas proportional counter whose resolution depends on the square root of the photon energy.
3. Combine the IBEC measurement with the calorimeter measurements, since provisional calculations suggested that a good IBEC experiment would determine the Q-value precisely.

Consequently it was decided to combine the calorimeter experiments with each of the four IBEC experiments. Figure 3 shows schematically these

eight experiments. The ninth is, of course, the calorimeter experiment alone.

This work has resulted in the development of a major part of the software for ongoing experiments at CERN and Aarhus.

0.2. Techniques.

Each spectrum that had to be generated was produced by standard monte carlo techniques. The 4p spectrum has a pole term which contains some 95% of the events. Therefore slightly different techniques were used in order to save computer time. Details are best found by looking at the source codes of I4PF and I4PV, the two relevant monte carlos. (The listings of all the programs take up some three inches of printout and so cannot be attached in an appendix. Instead they are available in B. Jonson's office at CERN in two files.)

The generated spectra were then fitted using standard chi-squared minimization techniques. A development version of MINUIT was used because it was found to converge more reliably (Filename: DL.JAM.MINSDBL). It is appropriate here to acknowledge that many of the subtleties of high precision fitting were explained by F. James, without whose advice this work would not have been successful. Three different chi-squares were defined:

$$\chi_1^2(m_\nu) = \sum_{i=1}^{N} \frac{(\text{Theory}(m_\nu)_i - \text{Experiment}_i)^2}{\text{Experiment}_i} \qquad (4)$$

$$\chi_2^2(m_\nu) = \sum_{i=1}^{N} \frac{(\text{Theory}(m_\nu)_i - \text{Experiment}_i)^2}{\text{Theory}(m_\nu = 0)_i} \qquad (5)$$

$$\chi_3^2(m_\nu) = \sum_{i=1}^{N} \frac{(\text{Theory}(m_\nu)_i - \text{Experiment}_i)^2}{\text{Theory}(m_\nu)_i} \qquad (6)$$

The differences are in the way the variance is defined. They were used in the following way:

1. χ^2_3 is used to determine the true value of the neutrino mass. (ie the value assumed by the source monte carlo.) This is done by plotting χ^2_3 versus m_ν. The curve should be parabolic with a minimum at the true value.

2. χ^2_2 is used to determine the probability that the value of m_ν at the minimum is greater than zero. $\Delta\chi^2_2(m_\nu)=\chi^2_2(m_\nu)-\chi^2_2(m_\nu=\text{min})$ is distributed as the chi-square distribution for one degree of freedom assuming that the neutrino mass is zero. This distribution is shown in table VI.
3. χ^2_1 is used in fitting the IBEC spectra initially in order to find an approximate solution. It's value is that it is more stable when the starting values of the parameters differ significantly from the values at the minimum. This is so because the end-point of the spectrum depends on Q and m_ν and the detector resolution in a complex way and all are being changed during the fitting process. As a result the variance defined from the theoretical spectrum changes also during the fit, thereby making the fitting process unstable. This instability goes away if the variance is defined by the experimental data, which does not change during the fit.

When this function has been minimized, the variance defined by the theoretical spectrum at this minimum is sufficiently close to the true one that it is then used to achieve the true minimum. Because it is sufficiently close to the true spectrum it is not changed during the second stage of the fit. So the fits are not unstable at any stage. This technique is not necessary to fit the calorimeter data because the energy levels of ^{163}Ho are known precisely from x-ray data. The fits to the calorimeter data are therefore intrinsically more stable and in practice easier to make. It is therefore possible to start the fit by minimizing χ^2_3 for the calorimeter data even when the starting values are 10% from the fitted values.

Whilst the difference between χ^2_2 and χ^2_3 is generally small, in practice it is significantly different from χ^2_1, which can also yield incorrect values for the true value of the neutrino mass. Note that the true values for Q and m_ν were taken to be 2580 and 30 eV respectively throughout.

The other important point is that the chi-square definitions in equations (4), (5) and (6) assume that the variance, however it is defined, is normally distributed. This is true if there are a large number of counts per bin. But this is not true in the tails of the distributions. The program was therefore written to sum the counts in adjacent bins until the number exceeded a certain threshold (15 counts per bin) and to integrate the theoretical spectral shape over the range of bins summed. In practice this involves some pattern recognition and is quite complex to code. Appendix A shows the flow diagram for this process. More details can be obtained from the files in Jonson's office.

0.3. Assumptions.

In the calorimeter experiments it was assumed that:

1. The detector resolution function was normally distributed and that σ_{det} was independent of energy.
2. The natural line widths were well known to, say, 0.1 eV.
3. The energy calibration was known absolutely.
4. There was no flat background.
5. There was no low energy detector background above a certain threshold (eg 1250 eV).
6. The trigger on the 25.65 keV gamma ray in ^{161}Ho rejected all backgrounds.
7. There was no pile-up.

In the IBEC spectra it was assumed that:

1. The five assumptions above applied except that:
   a. The detector resolution varied as $\sqrt{E}$ for those experiments using gas proportional counters.
   b. The threshold in point 5 above was 400 eV.
2. The fine structure due to $np_{1/2}$ and $np_{3/2}$ splitting was ignored, even though it is shown in figure 4.
3. That the trigger on 3p and 4p bremsstrahlung was 100% efficient with 100% efficient background rejection.
4. In practice the 4p spectrum will be contaminated with the $4D_{3/2}$ spectrum. This was omitted.
5. The photon passed through a 1/4 micron (over optimistic) mylar foil (see apparatus III in figure 1) at an angle Θ and the associated attenuation is given by (see reference [2]):

$$I = I_0 \exp(-\mu \rho x) \qquad (7)$$

where

$$\mu = 1.55 \left[\frac{12396}{E(eV)}\right]^{2.5065} \quad cm^2/g \qquad (8)$$

$$\rho = 1.39 \quad g/cm^3 \qquad (9)$$

$$x = \frac{t}{\cos\theta} \qquad t = .25\ \mu \qquad (10)$$

and $$-1 \leq \cos\theta \leq 1 \qquad (11)$$

6. The fitting program took the transmitted spectrum as having the form:

$$P(E) = \int_0^1 p(E, \cos\theta)\, d\cos\theta = \int_0^1 \exp(-a/\cos\theta)\, d\cos\theta$$

$$= \int_1^\infty y^{-2} \exp(-ay)\, dy$$

where $a = \mu(E)\rho t$

$$= e^{-a} - a\,Ei(-a) \qquad (12)$$

where Ei(-a) is the exponential integral of (-a).

7. The constants in equation (8) were assumed to be known absolutely, where as in practice two of them may be only accurate to about 5%. This could be a serious problem for thicker windows.
8. The data files, detector resolutions and the number of events in the fitted spectra are given in table IV. The "fractions transmitted" is the fraction of the events passing through the mylar window. The number of events generated can be calculated by dividing the number in the spectrum by the fraction transmitted. The time estimated to collect this data is estimated in table V.
9. Assumptions more specific to each fit will be given below.

0.4. Results.

1. ^{163}Ho calorimeter experiment (apparatus I): The data and fit for this experiment are shown in figure 5. The starting values for the fit are shown in figure VII for MINA2C. (Starting values for all

subsequent fits are given in table VII.) The results of the fits are given in table IX. The ratios R_1 and R_2 are defined as in equations (2) and (3) above. The ratios ΔR_i are defined by:

$$\Delta R_i = \frac{R_i^{Fit}}{R_i^{true}} = 1 \quad \text{for a perfect fit} \qquad (13)$$

We note that for this number of events (7×10^7 from table IV) the fitting error is of the order that required from table 1.

2. ^{161}Ho calorimeter experiment (apparatus II): The data and fit (MINA2BC) for this experiment are shown in figure 6. The results of the fits are shown in table IX. The results from these two experiments may be combined (program MINR) to determine Q and m_ν The fitted values of R_1 and R_2 are plotted in figure 2 (cross). The Q-value has been determined quite accurately (to about 1 eV) but the neutrino mass less so (to only about 25 eV) in agreement with table 1.

The running times for these two experiments are given in table V. They are 8.1 years and fourteen times 7.4 hours. The ^{161}Ho experiment is a logistical nightmare, in view of the short half-life. It would appear to be just about feasible to inject 10^{10} ^{161}Ho atoms into a solid state detector (see table III). But to do that 14 times seems incredibly complex. Furthermore pile-up may be a problem in the ^{161}Ho experiment.

It is for reasons such as these that we turned to investigate the IBEC spectra and the combined (or global) fit to all three types of experiment. We limited ourselves to 10^7 events in the calorimeter experiments for the global fit in order to reduce the running time to 1.2 years in the ^{163}Ho calorimeter experiment and two trips to Aarhus for the ^{161}Ho experiment. The Aarhus group have succeeded in implanting ^{163}Ho into a solid state detector. Preliminary data is shown in figure 7. The spike at 3.5 keV is a time calibration pulse. The resolution is clearly a lot better than the 200 eV assumed in our monte carlos. The low energy noise is also essentially zero above only 320 eV, which is very impressive. As a result the N_1 line can be clearly resolved. Some of the global fits assume that you can only fit the two M lines (eg GL23PF) above 1250 Volts, whilst others use this result to fit the three lines above 320 eV (eg GL33PF). Unfortunately the first detector built by Aarhus ran for only a few

tens of hours, which, whilst adequate for the ^{161}Ho experiment, is not good enough for the ^{163}Ho experiment.

3. MI3PF. 3p IBEC spectrum with a solid state detector (energy resolution "fixed" with energy). The data and fit for this experiment are shown in figure 8. The $\Delta\chi^2$ distribution for this experiment is shown in figure 9. The minimum is at 20 eV instead of 30 eV. From table XI the probability that $m_\nu = 0$ for $\Delta\chi^2=0.5$ is greater than 32%. So the result has no statistical significance even after taking data for 25.2 years.

4. GL23PF. This combines the data from MI3PF with the two calorimeter experiments. The data sets fitted are given in table IV. The program used the FCN subroutines from MINA2C, MINA2BC and MI3PF as subroutines for a global FCN (the function subroutine in MINUIT) which calculated all the parameters in terms of a single value for Q and a single value for m_ν . The three contributions to the χ^2 were summed. The result is shown in figure 9 and the statistical significance has clearly increased. But the probability that m_ν is really 0 eV (instead of 30 eV at the minimum) is still 2.5%, which is uncomfortably large. It is not a definitive experiment.

   Figure 10 shows $\Delta\chi^2_1$ for GL33PF. This is not a very satisfactory "parabola". It is not quite clear why the points at m_ν = 20 and 30 eV are so high. It is probable that these are false minima produced by MINUIT. Further computing could have resolved this problem. But lack of computing time prevented it. It would be quite reasonable if this were so because one would expect greater statistical accuracy from including the third line (ie shifting the threshold from 1250 eV in GL23PF to 320 eV in GL33PF). Unfortunately we cannot specify how much more significant because we do not know what the chi-square was at the true minimum.

5. MI3PV. This is the same as MI3PF except that now the detector resolution varies as $\sqrt{E}$. The data and fit above a threshold of 400 eV is shown in figure 11. Both χ^2_1 and χ^2_2 are shown in figure 12. They decrease as m_ν increases. If this was a real effect then it would not be possible to do the experiment with a gas proportional counter. $\Delta\chi^2_3$ shows the same trend in figure 13 except that it has a narrow minimum at the correct value of m_ν . (The black arrow in these figures indicates the true value of m_ν assumed in the monte carlo.) A more reasonable "parabola" is shown in figure 14. It was obtained by fixing the detector resolution. (Incidentally certain parameters were fixed in each of these fits. They are specified in table VII.)

This peculiar effect was not investigated further at that time. Subsequently it was found for the 4p spectra that the variable energy resolution had to be folded into the spectra using an integration which had to be done by 32 and 48 point Gaussian Quadrature to achieve sufficient precision. The integration is:

$$Th(k) = \int_a^b \frac{1}{\sigma(t)} \exp\left(-(k-t)^2/2\sigma^2(t)\right) f(t)\, dt \qquad (14)$$

where f(t) is the theoretical shape versus t (which is equivalent to the photon momentum except that it is here the variable of integration) before the resolution is folded in. $\sigma(t)=c\sqrt{E}$ where c is about 3 but has to be determined by the fit. This method of integration was never implemented in MI3PV because it seems unlikely that that experiment will ever be done and time was limited.

6. GL23PV. This program exists but is not debugged because of the problems with MI3PV.
7. MI4PF. This is the 4p spectrum using a solid state detector. The monte carlo data and fit are shown in figure 15. The plot starts at 400 eV, which corresponds to the threshold in the fitting program. The long plateau is curving down at low energies because of attenuation in the mylar window (see apparatus III, figure 1). The peak around 1840 eV is broadened by the detector resolution. This resolution was assumed to be 70 eV (165 eV FWHM). There are 10^8 events in this plot and the statistical precision is so great that in places the error bars hardly exceed the width of the line tracing the fitted curve. The $\Delta\chi^2$ curves from the fits are shown in figure 16. $\Delta\chi^2_1$ gives a minimum at 50 eV and $\Delta\chi^2_2$ a minimum at 40 eV. Only $\Delta\chi^2_3$ gives the minimum at the true value of 30 eV, as explained above. The probability that the mass is zero can be found from the $\Delta\chi^2_2$ distribution, which is 11.9 between 0 and 30 eV. From table VI this corresponds to a probability that the mass is zero (and not 30 eV) of 0.05%, which would be a meaningful result.

A few words about the set-up are appropriate. In practice it would not look exactly like apparatus III in figure 1 because it is not possible to build large area silicon detectors with such good resolution. A monoatomic layer of 10 μg of ^{163}Ho occupies a source area of 36 cm². A typical silicon detector would have a sensitive area of 2 cm² or less. As a result, somewhere between 10 and 20 such

detectors would be required to collect 10^8 events in 1.4 years. There would probably be problems matching the data from the different detectors because of differences in the energy calibrations. If these problems can be resolved (as has been assumed here) then this is the best experiment simulated.

8. GL34PF. The $\Delta\chi^2_2$ distribution for the above data combined with calorimeter data is also shown in figure 16. The $\Delta\chi^2_2$ is 11.8 so that the statistical significance does not seem to have improved.

9. MI4PV. This experiment is similar to that discussed in point 7 above except that the detector is a gas proportional counter whose resolution varies as $\sqrt{E}$. At 2 keV this gives σ_{det} = 133 eV (or 313 eV FWHM), which is nearly double that of solid state detectors previously considered. This broadens the spectrum significantly as can be seen by comparing figures 15 and 17.

Figures 17,18,19 and 20 show the same data fitted assuming that the neutrino mass is 0, 20, 40 and 60 eV respectively. (The true value being 30 eV.) The end-point moves hardly at all. The change in shape can only be seen by taking the originals from 0 and 60 eV, over-laying them and holding them up to a bright light.

The fitting program used the Gaussian quadrature integration, as mentioned above, to fold the resolution into the spectrum. The minimum 16 points were used and this was increased to 32 points and then to 48 points as the χ^2 fell below certain levels in order to reduce computing time. (It was later realized that it is not clear that this saves time unless MINUIT is informed of the change, which it was not.) This program (and the associated one GL34PV) used enormous amounts of computing time (80 and 120 minutes respectively for one point). And this was with MINUIT in a truncated mode. That is to say, the minimum number of iterations through FCN was limited to 120. Without this cut MINUIT could go on for hours without satisfying its internal convergence criteria. (Whether these were appropriate to the problem in hand is not clear.) Never-the-less it seemed to have reached some plateau in chi-square after 120 iterations and so it was assumed that this was the minimum. The odd bumps in the $\Delta\chi^2$ distributions in figures 21, 22 and 23 suggest that this was only approximately correct.

The $\Delta\chi^2_2$ distribution is shown in figure 21. The minimum is not at 30 eV as might be expected. $\Delta\chi^2_3$ distribution was not run because of lack of computing time. It is therefore an assumption that this experiment would yield the true neutrino mass.)

If we take the true value as 30 eV then the probability that the

mass is not zero is 2.5% (from $\Delta\chi^2_2$=5). This is not nearly as meaningful as the solid state detector experiment (MI4PF) and presumably reflects the effects of worse detector resolution and possible effects of having it vary as $\sqrt{E}$.

Provisional trials showed that the fit was extraordinarily sensitive to the widths of the M_1 and N_2 levels, which determine the width of the line at 1840 eV. A version of the program MI4PV was therefore produced in which Γ_{M_1} and Γ_{N_2} were free variables. The $\Delta\chi^2_2$ and the $\Delta\chi^2_3$ distributions for this program are shown in figure 22. The $\Delta\chi^2_3$ distribution has a minimum at the true mass (30 eV). (The point at 20 eV is a bit high, perhaps because the fit has not properly converged.) But the probability that the mass is zero has risen to 15% ($\Delta\chi^2_2$= 2.3), which, of course, is completely unsatisfactory.

(Note that if we allow Γ_{M_1} and Γ_{N_2} to be free parameters in MI4PF, as is probably necessary, and assume that the $\Delta\chi^2$ is reduced by 3 as here, then the probability that the neutrino mass is zero rises from 0.05% to 0.3%.)

It is perhaps of interest that these fits yield extraordinarily precise values of these widths, to about 0.1 eV, assuming absolute energy calibration. This would be an interesting physics result in its own right, since there is no precise experimental data on the widths of M and N shell lines.

Finally, figure 23 shows $\Delta\chi^2$ versus Q. In this figure the procedure was reversed. Instead of running MINUIT with Q as a variable and m_ν fixed at each of the values in turn plotted in figure 21, say, m_ν was a variable and Q was fixed at the values plotted in figure 23. A shift of 1 volt in the Q-value produces a $\Delta\chi^2$ of 50 or more. Thus, from the statistical point of view, it should be possible to determine Q very precisely. There will inevitably be problems with energy calibration. It is my opinion, based on intuition, that the 4p spectrum will be self-calibrating in energy because it is dominated by a pole term whose position is determined by atomic energy levels which are known to a fraction of a volt. So although the energy self-calibration has not yet been simulated (The program modifications can be made relatively easily.) it is quite likely that it is no real problem.

0.5. Limits on the Neutrino Mass.

It seems highly unlikely that any of the simulated experiments described above are going to be the definitive neutrino mass experiment. Never-the-less we have shown that the Q-value can be determined quite precisely, which will be useful in designing future experiments. It is also possible to place a limit on the neutrino mass.

You can see from table VI that a confidence level of 95% corresponds to a $\Delta\chi^2$ of 4. From figure 21 (Γ_{M_1} and Γ_{N_2} fixed) the limit is about 60 eV at the 95% confidence level. And from figure 22 (Γ_{M_1} and Γ_{N_2} variable) it is about 65 eV. No doubt that by the time other effects of reality are included (eg backgrounds, energy calibration, etc) these limits will rise. But it seems very likely that they will be of order of or less than 100 eV, which is a good start.

0.6. Alternatives.

The objective of this work was to design a neutrino mass experiment using ^{163}Ho that was truly competitive with or superior to any other neutrino mass experiment, running or proposed. It may still be possible to achieve this goal because some of the more interesting possibilities have yet to be considered. The main lesson to be drawn from this study is that the detector resolution must be better than the mass limit sought. In other words if you plan to put a limit in the region of 30 eV you need a detector with a resolution of 3 to 10 eV at most. Table VIII gives some information on the Livermore tritium experiment, which deploys a frozen tritium source. (The solid angle is a guesstimate and may be wrong.) Table X gives details on four more experiments. The Livermore experiment is the only one with a resolution below 10 eV (claimed). The author believes that the CERN group should aim to do a similar experiment with ^{163}Ho as soon as possible.

Is this possible? I believe that it may be because there exist two promising categories of experiment which I have not had time to model. The theoretical details of one of these have been discussed in references [3] and [4]. This is to measure the end-point shape in the single electron capture spectrum (SEEEC):

$$^{163}Ho \rightarrow {}^{163}Dy^{H_1\,H_2} + e^- + \nu_e \qquad (15)$$

This very complex spectrum is shown in figure 24 and the end-point shape in figure 25. (A full explanation of these figures is given in reference [4].)

It is relevant here to mention that De Rujulla's original paper stressed the bremsstrahlung spectra. Whilst these are interesting physics, the rates are too low and it seems impossible to build x-ray diffractometers with energy resolutions better than 10 eV and transmission efficiencies better than 10^{-5}. Furthermore the source strengths are weak because the lifetime of ^{163}Ho is 640 times that of tritium and you get fewer atoms per gram (1/54th the number to be exact). The tendency of the group has been to explore large acceptance photon detectors with poor energy resolution. I believe this is an error, which I fell into also. It is almost certainly very desirable to consider the electron spectra because:

1. The branching ratio to electrons is of order 1000 times that to photons.
2. Electron spectrometers can have large acceptance and high resolution.

It is worth noting that ^{163}Ho has certain advantages over tritium:

1. The Q-value is about one seventh.
2. The Q-value can probably be determined more precisely in absolute terms than for tritium. This is important in estimating the number of missing events.
3. Larger solid angle spectrometers can probably be built for the lower electron energies.

Just to stimulate the thinking within the group, it is worth noting that the integral spectrum can perhaps be measured with a cylindrical system as shown in figure 26. A retarding potential on a grid, regulated to one volt (1:2500), prevents electrons with energy less than the grid potential from reaching the detector. Such a system could conceivably have a 2π solid angle for a 1mg (0.5 mCu) source of holmium. This would give 80 "missing" events per day. The detector should have very low noise and determine the electron energy reasonably well so that noise pulses corresponding to the wrong energy can be eliminated. Cosmic rays can be vetoed and pre-World War II lead can shield against natural low energy backgrounds. If you could get backgrounds from all sources down to a few events per day in a 50 eV wide region around the end-point, which does not seem implausible, then you have a viable experiment. In principle.

In practice you might find that the energy selectivity of the grid was compromised by the range of incident angles. (And don't forget that the solid angle is effectively reduced by the retarding voltage on the grid.) This could be solved by putting in a collimator, which would reduce the

solid angle. You would also find it difficult to build a cyclindrical outer electrode and detector combined. This could be resolved by using a separated function system: cyclindrical grids form all electrodes and flat or cylindrical detectors surround them.

A parallel plate capacitor system with separated functions and collimator is shown in figure 27. It would have a smaller solid angle than the cyclindrical system in figure 26 but it would be simpler to build. In fact it might be possible to build something in a few months. And this perhaps is the real advantage of ^{163}Ho. The Livermore tritium experiment is technically quite a challenge. (The system also measures the integral spectrum but is over 20 m long, I believe. Clearly the retarding voltage must be maintained to one part in 10^4 or better.) It is estimated that it will take 2 years to get running. So if CERN could get a high resolution system running a year sooner, the lower counting rate might not prevent CERN from obtaining the first results. In fact if the Q-value is found to be 2300 volts instead of 2580 then the g value will increase by an order of magnitude and hence the counting rate.

The second method is unique to ^{163}Ho. ^{163}Ho has decay modes that throw off several electrons as discussed in reference [3]. If you view ^{163}Ho through a retarding potential of order -1250 volts then you see only two such modes involving pairs of electrons for energetic reasons. They are:

$$^{163}Ho \rightarrow {}^{163}Dy^{H_1 H_2} + e_1^- + \nu_e$$
$$\hookrightarrow {}^{163}Dy^{H_1' H_1'' H_2} + e_2^- \quad (H_1 \rightarrow H_1' H_1'') \qquad (16)$$

In the first case $H_1H_2 = M_5N_{67}$ and $H_1 \rightarrow H'H'' = M_5 \rightarrow N_{67}N_{67}$. The end-point is at 1281 eV and the energy of the monochromatic electron is 1287 eV. In the second case $H_1H_2 = M_4N_{67}$ and $H_1 \rightarrow H'H'' = M_4 \rightarrow N_{67}N_{67}$. The endpoint is at 1243 eV and the energy of the monoenergetic electron is 1324 eV.

In each case one electron is a line (e_2) and the other has a continuous spectrum out to the end-point. In each event the time separation of the monoenergetic electron and the electron from the continuous spectrum can be calculated from the latter's energy. It is thus a coincidence experiment with essentially no background problems, or at least much lower ones than in the other neutrino mass experiments. And if the energies of both

electrons are measured as well as the relative time-of-flight then each event is over-determined. This, together with the low energies involved, is unique to ^{163}Ho and perhaps for this reason deserves more attention than other methods. At these low energies electrostatic spectrometers can be built with larger solid angles than magnetic ones. Or, the effective solid angle might be increased by accelerating the electrons first and then using a magnetic spectrometer. Charpak [5] has designs for a detector with good spacial resolution for two particles and which can measure their relative timing to 100 picoseconds. This is more than adequate.

A possible set-up is shown in figure 28. This experiment would also benefit from knowing the Q-value. McGuire at Sandia Laboratories, Albuquerque, New Mexico, has expressed interest in calculating the angular distributions for these pairs of electrons, which perhaps should be known if a detailed design study is to be made.

0.7. Conclusions.

The calorimeter data can be fitted, in principle, with the required precision. But the precision in mass is not very great, even after running one experiment for eight years and repeating the other, at great logistical difficulty, fourteen times. Furthermore a simplified program does not improve the results of one of the IBEC experiments significantly. Maybe the Aarhus work will yield in good time a better value for Q. Otherwise it does not seem worth continuing. This seems unfortunate in view of the impressive technical progress. There may be factors the author is unaware of which reverse this opinion.

The best IBEC experiment simulated is for the 4p spectrum using a solid state detector (MI4PF). This could give a positive result for a neutrino mass of 30 eV with a probability that it was zero in the range 0.05% to 0.3%. However, fitting the data would not be easy. There would always be potential problems matching the data from several detectors. So people could always have reasonable doubt that the results of the fits were correct. Thus even if the result was correct it would not be convincing. And conviction is everything. This problem can only be overcome, in the author's opinion, by going to detectors with resolutions better than the mass to be determined. In fact it has been pointed out [6] that it is then possible to measure the curvature of the curie plot at the end-point. And this is different for a spectrum distorted by the detector resolution than for the down turn produced by a finite neutrino mass.

The second best IBEC experiment simulated is that which measures the 4p spectrum using a gas proportional counter (MI4PV). This experiment

does not resolve a neutrino mass of, say, 30 eV. But it does yield a precise value for Q (as would the other 4p experiment MI4PF) to a few volts and enables one to put a limit on the neutrino mass of order 100 eV.

There are of course reservations about these experiments concerning the ability to trigger on 4p spectra, which can only be resolved by experiment. Further work with these programs would test whether fitting the fine structure or the $4D_{3/2}$ component were also problems. These experiments would also determine the widths of the M_1 and N_2 lines very precisely as a by-product. This is very interesting from the point of view of atomic physics.

There are very good reasons to believe that the definitive neutrino mass experiment with ^{163}Ho will involve electrons and not photons. And the detector will be some kind of electrostatic spectrometer with an energy resolution of a few volts. For example a simple system such as that shown in figure 27 may collect as many as 10 'missing' events per day in an integral spectrum. And it may be possible to build it quite quickly. The low Q-value of ^{163}Ho is a unique advantage as is the possibility of doing coincidence measurements. The first group with data with a resolution of a few volts is going [1] to be taken very seriously by the physics community. It is therefore worth every effort to achieve such a goal.

0.8. Acknowledgements.

I should like to thank A. De Rujulla, B. Jonson, H. Ravn, G. Charpak, F. James, J. J. Simpson, G. Erskine, R. Cool and D. Anderson for useful discussions. I thank M. Izycki for writing plotting subroutines. I thank CERN for its hospitality that made this work possible.

References

[1] A. De Rujulla. Nuc. Phys. B188(1981), 414.

[2] George L. Clark, ed. "Encyclopaedia of x-rays and gamma rays". Reinhold Publishing Corp. New York.

[3] A. De Rujulla and M. Lusignoli. "Venerable, Embryo and Future Methods to Measure Electron Neutrino Masses". Th.3300-CERN (1982).

[4] A. De Rujulla and M. Lusignoli. "Single Electron Ejection in Electron Capture as a tool to Measure the electron Neutrino Mass". Th.3444-CERN (1982).

[5] G. Charpak. Private communication.

[6] J. J. Simpson. CERN Particle Physics Seminar, 1982.

Table captions

Table I. Estimate of the precision of the calorimetric method.

Table II. Electron capture lines in holmium.

Table III. ^{161}Ho source strength estimates.

Table IV. Data files used by programs and related files.

Table V. Counting rates in various experiments and running times.

Table VI. The chi-squared distribution for one degree of freedom.

Table VII. Starting parameter values for MINUIT and list of fixed parameters.

Table VIII. Comparison of the Livermore Tritium experiment and a possible ^{163}Ho experiment.

Table IX. Results of fits to the calorimeter data.

Table X. Comparison of beta spectrometers for tritium experiments.

Table I

δQ	δR^{o}_{NM}	δR_{NM}	Q=2480 δm_ν	Q=2580 δm_ν	Q=2680 δm_ν
1eV	0.1%	0.1%	13eV	16eV	19eV
2	0.2	0.2	26	32	39
4	0.4	0.4	51	64	78
5	0.5	0.5	64	80	97
5	1.0	1.0	75	101	131

Table II

Line	Energy (eV)
M_I	2046.8
M_{II}	1841.8
N_I	416.3
N_{II}	331.8

Table III. ^{161}Ho Source Strength.

Transfer from separator to hot lab:	10 min
Chemical separation:	120 " ?
Transport to airport:	60 "
Flight time to Copenhagen:	175 "
Transfer to Aarhus plane:	120 " ?
Bus to Aarhus:	45 "
Flight to Aarhus:	30 " ?
Loading of the ion source:	15 "
Pumping of the ion source:	30 " ?
Implantation:	30 " ?
Mount detector:	30 " ?
Start counting after:	665 "
	~11 hours

^{161}Ho source strength:	
$T_{\frac{1}{2}}$ = 2.5 h. Purity before implantation:	10^{-8}
ISOLDE production rate	10^{10} atoms/sμA
Impurity level:	10^{-4}
10 hour collection:	8×10^{13} atoms
Chemical separation efficiency of .5:	4×10^{13} "
Transport to Aarhus:	2.5×10^{12} "
Implantation efficiency of .005	1.3×10^{10} "

Start counting with 10^{10} atoms in detector.

Table IV: Data files used by programs and related parameters.

Program	Figure No.s	Files	Detector Resolution (eV)	Number of events	Fraction transmitted	Apparatus
MINA2C	5	ECPHA277	200	7×10^7	-	I
MINA2BC	6	ECPHB277	200	7×10^7	-	II
MI3PF	8,9	I3PF61	100	2.8×10^5	.281	III
GL33PF	9,10	I3PF61	100	2.8×10^5	.281	III
		ECPHA2E7	200	1×10^7	-	I
		ECPHB2E7	200	1×10^7	-	II
MI3PV	11,12,13,14	I3PV67	$3\sqrt{E}$	2.8×10^5	.281	III
GL23PV	-	I3PV67	$3\sqrt{E}$	2.8×10^5	.281	III
		ECPHA2E7	200	1×10^7	-	I
		ECPHB2E7	200	1×10^7	-	II
MI4PF	15,16	I4PFZ82	70	1×10^8	.869	III
GL34PF	16	I4PFZ83	70	1×10^8	.869	III
		ECPHA2E7	200	1×10^7	-	I
		ECPHB2E7	200	1×10^7	-	II
GL34PV	21	I4PV87	$3\sqrt{E}$	1×10^8	.869	III
		ECPHA2E7	200	1×10^7	-	I
		ECPHB2E7	200	1×10^7	-	II
MI4PV	17,18,19,20, 21,22,23	I4PV87	$3\sqrt{E}$	1×10^8	.869	III

Table V. Counting Rates.

Apparatus I: ^{163}Ho.

source	lifetime	decays/s	Branching Ratio	$\Delta\Omega/4\pi$	coincidences per second	Running time	Number of events
10^{11} atoms	8000 yrs.	0.274	1.	100%	.274	1.2 yrs	10^7
						8.1 yrs	7×10^7

Apparatus II: ^{161}Ho.

10^{10} atoms	2.48 h.	7.6×10^5	0.009*	5%	350	7.4 h.	4.5×10^6
						Two runs to get 10^7 events.	
						14 " " " 7×10^7 events.	

Apparatus III: IBEC.

10 μg	8000 yrs.	10^5	$3p=1.2\times10^{-7}$	10%	1.3×10^{-3}	25.2 yrs	2.8×10^5
			$4p=2.6\times10^{-4}$	10%	2.7	1.4 yrs.	1×10^8
Same but X-ray spectrometer:			$4p=2.6\times10^{-4}$	10^{-5}	2.7×10^{-4}	1.4×10^4	1×10^8

* Branching ratio for 25.65 keV gamma is 25% and for M & N shell lines is 3.62%.

Table VI. Chi-squared distribution for one degree of freedom.

PROBABILITY	$\Delta\chi^2_2$
0.3173D+00	0.1000D+01
0.1573D+00	0.2000D+01
0.8326D-01	0.3000D+01
0.4550D-01	0.4000D+01
0.2535D-01	0.5000D+01
0.1431D-01	0.6000D+01
0.8151D-02	0.7000D+01
0.4678D-02	0.8000D+01
0.2700D-02	0.9000D+01
0.1565D-02	0.1000D+02
0.9111D-03	0.1100D+02
0.5320D-03	0.1200D+02
0.3115D-03	0.1300D+02
0.1828D-03	0.1400D+02
0.1075D-03	0.1500D+02
0.6334D-04	0.1600D+02
0.3738D-04	0.1700D+02
0.2209D-04	0.1800D+02
0.1307D-04	0.1900D+02
0.7744D-05	0.2000D+02
0.4593D-05	0.2100D+02
0.2727D-05	0.2200D+02
0.1620D-05	0.2300D+02
0.9634D-06	0.2400D+02
0.5733D-06	0.2500D+02
0.3414D-06	0.2600D+02
0.2035D-06	0.2700D+02
0.1213D-06	0.2800D+02
0.7238D-07	0.2900D+02
0.4320D-07	0.3000D+02
0.2580D-07	0.3100D+02
0.1542D-07	0.3200D+02
0.9216D-08	0.3300D+02
0.5511D-08	0.3400D+02
0.3297D-08	0.3500D+02
0.1973D-08	0.3600D+02
0.1181D-08	0.3700D+02
0.7074D-09	0.3800D+02
0.4238D-09	0.3900D+02
0.2540D-09	0.4000D+02
0.1522D-09	0.4100D+02
0.9127D-10	0.4200D+02
0.5474D-10	0.4300D+02
0.3284D-10	0.4400D+02
0.1970D-10	0.4500D+02
0.1183D-10	0.4600D+02
0.7099D-11	0.4700D+02
0.4262D-11	0.4800D+02
0.2560D-11	0.4900D+02
0.1537D-11	0.5000D+02
0.9237D-12	0.5100D+02
0.5550D-12	0.5200D+02
0.3335D-12	0.5300D+02
0.2005D-12	0.5400D+02
0.1205D-12	0.5500D+02
0.7247D-13	0.5600D+02
0.4358D-13	0.5700D+02
0.2620D-13	0.5800D+02
0.1577D-13	0.5900D+02
0.9492D-14	0.6000D+02
0.5718D-14	0.6100D+02
0.3442D-14	0.6200D+02
0.2054D-14	0.6300D+02
0.1249D-14	0.6400D+02
0.7494D-15	0.6500D+02
0.4441D-15	0.6600D+02
0.2776D-15	0.6700D+02
0.1665D-15	0.6800D+02
0.1110D-15	0.6900D+02
0.5551D-16	0.7000D+02
0.2776D-16	0.7100D+02
0.2776D-16	0.7200D+02
0.0	0.7300D+02
0.0	0.7400D+02
0.0	0.7500D+02

Table VII. MINUIT Starting Parameter and Limits.

PGM = MINA2C.

HO 163. Q=2580 MNU=30 SDET=200 TIME 0.046

1	RMI	.130270D+08	50.0000	.0	.0
2	RMII	.131600D+07	50.0000	.0	.0
3	RNI	.527520D+08	50.0000	.0	.0
4	RNII	.290500D+07	50.0000	.0	.0
5	SDET	200.000	10.0000	150.000	250.000

PGM = MINA2BC

HO 161. Q=2580 MNU=30 SDET=200 TIME 0.030

1	RMI	.533680D+08	50.0000	.0	.0
2	RMII	.280700D+07	50.0000	.0	.0
3	RNI	.131530D+08	50.0000	.0	.0
4	RNII	672000.	50.0000	.0	.0
5	SDET	200.000	10.0000	150.000	250.000

PGM = MI3PF. Parameters 2,5 & 6 were fixed.

HO 163. Q=2580 MNU=30 SDET=200 TIME 0.034
MACH. PREC.=

1	Q163	2580.00	10.0000	2500.00	2700.00
2	MNU	30.0000	1.00000	.0	100.000
3	SDET	100.000	1.00000	90.0000	105.000
4	NORM	46.3000	.100000	.100000D-01	1000.00
5	ATTA	1.00000	.100000	.100000	20.0000
6	ATTP	1.00000	.100000	.500000	2.00000

Table VII (Cont'd)

GLOBAL FIT TO HO163/161(SDET=200) AND IBEC(SDET=100).Q=2580 TIME 0.032 MACH. PREC.=

1	RMI	6.50000	.100000	1.00000	10.0000
2	RMII	.350000	.100000	.100000	5.00000
3	RNI	1.60000	.100000	.100000	5.00000
4	RNII	.820000D-01	.100000D-01	.100000D-01	1.00000
5	Q163	2580.00	10.0000	2500.00	2700.00
6	MNU	30.0000	1.00000	.0	100.000
7	S163	200.100	10.0000	150.000	250.000
8	S161	200.000	10.0000	150.000	250.000
9	SBEC	100.000	1.00000	90.0000	105.000
10	N161	.150000	.100000	.100000D-01	100.000
11	NBEC	38.8000	.100000	.100000D-01	1000.00
12	ATTA	1.00000	.100000	.100000	10.0000
13	ATTP	1.00000	.100000	.500000	2.00000

PGM = GL23PF. Parameters 6,7,8,9,12 & 13 were fixed.

HO 163. Q=2580 MNU=30 SDET=200 TIME 0.043 MACH. PREC.=

1	Q163	2580.00	10.0000	2500.00	2700.00
2	MNU	30.0000	1.00000	.0	100.000
3	SDET	7.00000	.100000	5.00000	9.00000
4	NORM	40.0000	.100000	.100000D-01	1000.00
5	ATTA	1.00000	.100000	.100000	20.0000
6	ATTP	1.00000	.100000	.500000	2.00000
7	SIGP	1.00000	.100000	.500000	2.00000

PGM = MI3PV. Parameters 2,5,6 & 7 were fixed.

HO 163. Q=2580 MNU=30 SDET=200 TIME 0.032 MACH. PREC.=

1	Q163	2580.00	10.0000	2500.00	2700.00
2	MNU	.0	1.00000	.0	100.000
WARNING	- ABOVE PARAMETER IS AT LIMIT				
3	SDET	70.0000	1.00000	65.0000	75.0000
4	NORM	.360000D-02	.100000D-03	.100000D-03	1.00000
5	ATTA	1.00000	.100000	.100000	20.0000
6	ATTP	1.00000	.100000	.500000	2.00000

WARNING - VARIABLE 2 HAS BEEN BROUGHT BACK INSIDE LIMITS BY PINTF.

PGM = MI4PF. Parameters 2,5 & 6 were fixed.

Table VII (Cont'd)

```
*************************************************************************
 GLOBAL FIT TO HO163/161(SDET=200) AND IBEC(SDET=100).Q=2580       TIME   0.035
                                                                   MACH. PREC.=
*************************************************************************
*************************************************************************
      1         RMI     6.50000      .100000        1.00000      10.0000
      2         RMII    .350000      .100000        .100000      5.00000
      3         RNI     1.60000      .100000        .100000      5.00000
      4         RNII    .820000D-01  .100000D-01    .100000D-01  1.00000
      5         Q163    2580.00      10.0000        2500.00      2700.00
      6         MNU     30.0000      1.00000        .0           100.000
      7         S163    200.100      10.0000        150.000      250.000
      8         S161    200.000      10.0000        150.000      250.000
      9         SBEC    70.0150      1.00000        65.0000      75.0000
     10         N161    .150000      .100000        .100000D-01  100.000
     11         NBEC    .113000      .100000D-03    .100000D-03  1000.00
     12         ATTA    1.00000      .100000        .100000      10.0000
     13         ATTP    1.00000      .100000        .500000      2.00000
*************************************************************************
```

PGM = GL34PF. Parameters 6,7,8,9,12 & 13 were fixed.

```
*************************************************************************
 HO 163.  Q=2580   MNU=30   SDET=200                               TIME   0.029
                                                                   MACH. PREC.=
*************************************************************************
*************************************************************************
      1         Q163    2580.00      10.0000        2500.00      2700.00
      2         MNU     .0           1.00000        .0           100.000
WARNING          - ABOVE PARAMETER IS AT LIMIT
      3         SDET    7.00000      .100000        5.00000      9.00000
      4         NORM    .360000D-02  .100000D-03    .100000D-03  1.00000
      5         ATTA    1.00000      .100000        .100000      20.0000
      6         ATTP    1.00000      .100000        .500000      2.00000
      7         SIGP    1.00000      .100000        .500000      2.00000
*************************************************************************
WARNING - VARIABLE  2 HAS BEEN BROUGHT BACK INSIDE LIMITS BY PINTF.
```

PGM = MI4PV. Parameters 2,5,6 & 7 were fixed.

Table VII (Cont'd)

GLOBAL FIT TO HO163/161(SDET=200) AND IBEC(SDET=100).Q=2580 TIME 0.037 MACH. PREC.=

1	RMI	6.50000	.100000	1.00000	10.0000
2	RMII	.350000	.100000	.100000	5.00000
3	RNI	1.60000	.100000	.100000	5.00000
4	RNII	.820000D-01	.100000D-01	.100000D-01	1.00000
5	Q163	2580.00	10.0000	2500.00	2700.00
6	MNU	30.0000	1.00000	.0	100.000
7	S163	200.100	10.0000	150.000	250.000
8	S161	200.000	10.0000	150.000	250.000
9	SBEC	7.00000	.100000	5.00000	9.00000
10	N161	.150000	.100000	.100000D-01	100.000
11	NBEC	.125000D-01	.100000D-03	.100000D-03	1000.00
12	ATTA	1.00000	.100000	.100000	10.0000
13	ATTP	1.00000	.100000	.500000	2.00000
14	SIGP	1.00000	.100000	.500000	2.00000

PGM = GL34PV. Parameters 6,7,8,9,12,13 & 14 were fixed.

Table VIII: Comparison of a Tritium and a ^{163}Ho experiment.

Item	Tritium (Livermore)	^{163}Ho. (SEEEC) (CERN)	$\frac{^3H}{^{163}Ho}$
(eV)	2 to 3	2 to 3†	-
source	50 - 100 Cu 3.6-7.2 mg	0.5 mCu 1 mg	10^5
solid angle ($\Delta\Omega/4\pi$)	2×10^{-4}*	0.5	4×10^{-4}
g(m =30)	56×10^{-10}	$1 \times 10^{-10}$$^{+}$	56
missing events per day:	1.8×10^{5}*	80	2200

* May be less because of collimator.

† May be greater unless collimated.

$^{+}$ May be greater by factor of 10 if Q=2300 V.

Table IX: Fits to Calorimeter Data.

Parameter	^{163}Ho. True Value	^{163}Ho. Fitted Value	^{161}Ho. True Value	^{161}Ho. Fitted Value.
λ_{MI}	.1861	.1861	.7624	.7627
λ_{MII}	.0188	.01879	.0401	.03985
λ_{NI}	.7536	.7534	.1879	.1878
λ_{NII}	.0415	.04166	.0096	.009582
σ(eV)	200.	200.1	200.	200.0
ΔR_1	1.	1.0009	1.	1.0003
ΔR_2	1.	0.9943	1.	0.9997

Combined Result

	True Value	Fitted Value
R_1	.0607	.06057
R_2	.1164	.1162
Q(eV)	2580.	2579.1
m_ν(eV)	30.	7.16

Table X: Comparison of beta spectrometers.

Property	Stockholm	Moscow	Tokyo	Chalk River
Type	2	Toroidal	2	2
Radius (cm)	50	21.3	75	100
Momentum res.(%)	0.11	0.12	0.03	0.05
Source elements	85	18	?	180
Element height(cm)	10	1.8	?	10
" width (cm)	0.17	0.26	?	0.1
Total area (cm)	145	8.4	2	180
Transmission (%)	0.5	0.83	0.1	0.1
Dispersion (mm)	2000	3900	3000	4000
Det. slit width(mm)	2.	3.	2.*	1.
No. det. channels	1	3	60*	60
Overall res. FWHM(eV)	55	45	25*	19
Det. range (eV)	55	3*45	1450	1120

* Single wire proportional counter.

Figure captions

Figure 1. Schematic layouts of apparatus for simulated experiments.

Figure 2. Analysis of calorimeter data.

Figure 3. IBEC experiments simulated.

Figure 4. Various IBEC spectra.

Figure 5. Pulse height spectrum from ^{163}Ho.

Figure 6. Pulse height spectrum from ^{161}Ho.

Figure 7. Experimental pulse height spectrum from ^{163}Ho measured by Aarhus.

Figure 8. The 3p spectrum with a solid state detector.

Figure 9. $\Delta\chi^2$ distributions for MI3PF and GL23PF.

Figure 10. $\Delta\chi^2_1$ distribution for GL33PF.

Figure 11. 3p spectrum with a gas proportional counter as detector.

Figure 12. $\Delta\chi^2$ distributions for MI3PV.

Figure 13. $\Delta\chi^2_3$ distribution for MI3PV.

Figure 14. $\Delta\chi^2_2$ distribution for MI3PV with σ_{det} fixed during the fit.

Figure 15. The 4p spectrum with a solid state detector.

Figure 16. $\Delta\chi^2$ distributions for MI4PF and GL34PF.

Figure 17. The 4p spectrum with a gas proportional counter for m_ν=0.

Figure 18. The 4p spectrum with a gas proportional counter for m_ν=20.

Figure 19. The 4p spectrum with a gas proportional counter for m_ν=40.

Figure 20. The 4p spectrum with a gas proportional counter for m_ν=60.

Figure 21. $\Delta\chi^2_2$ distributions for MI4PV and GL34PV with Γ_{M_1} and Γ_{N_2} fixed.

Figure 22. $\Delta\chi^2$ distributions for MI4PV with Γ_{M_1} and Γ_{N_2} free.

Figure 23. $\Delta\chi^2$ distribution versus Q.

Figure 24. The single electron ejection elctron capture spectrum.

Figure 25. A calculation of the shape at the end-point of the SEEEC spectrum made by the authors of reference (4).

Figure 26. A provisional schematic layout for a cylindrical system for an SEEEC experiment.

Figure 27. A parallel plate condensor system for a SEEEC experiment.

Figure 28. A spectrometer system for the proposed two electron ejection electron capture experiment (TEEEC).

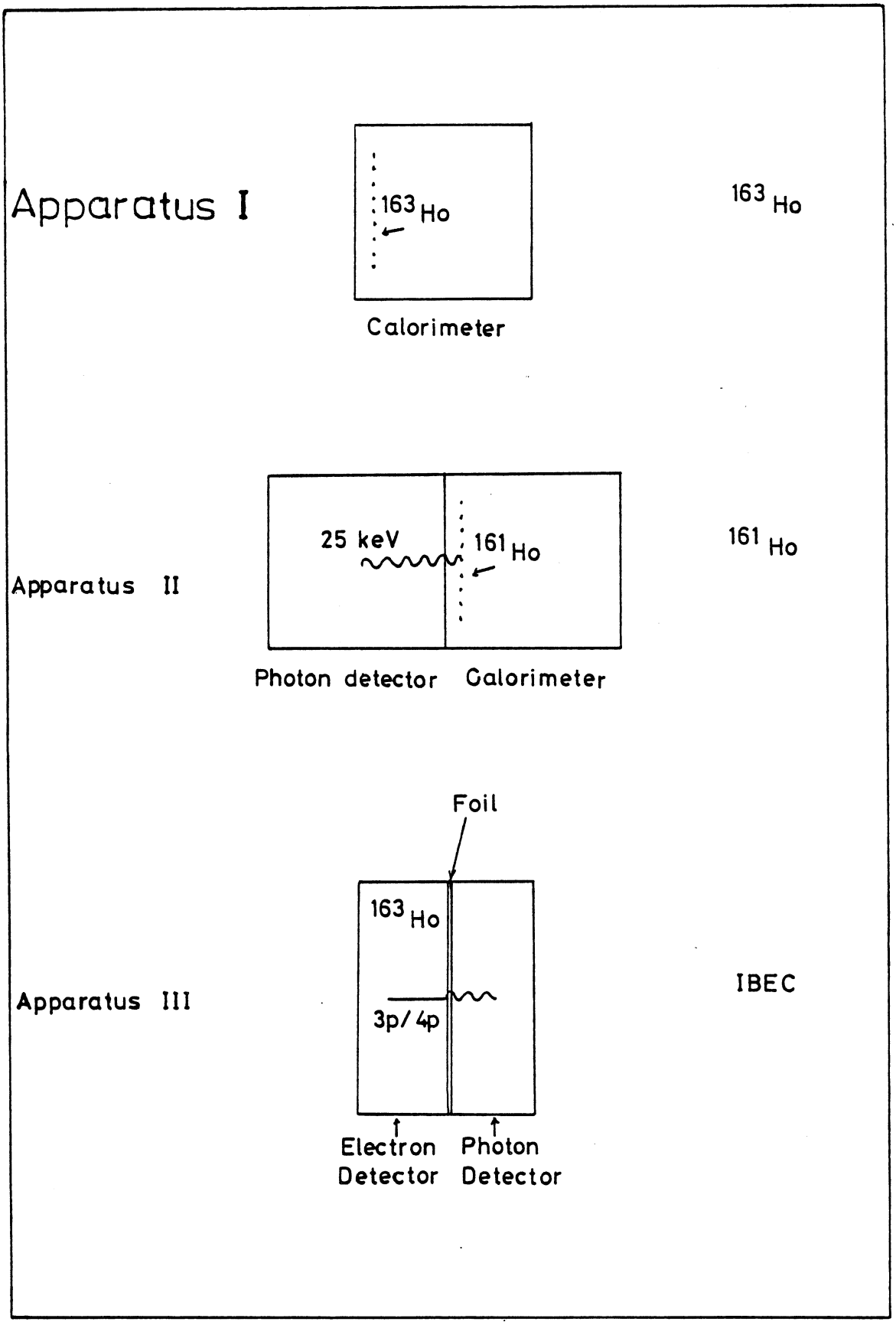
Apparatus I
163 Ho
Calorimeter
163 Ho
Apparatus II
25 keV
161 Ho
Photon detector
Calorimeter
161 Ho
Foil
Apparatus III
163 Ho
3p/4p
IBEC
Electron Detector
Photon Detector

Fig. 1

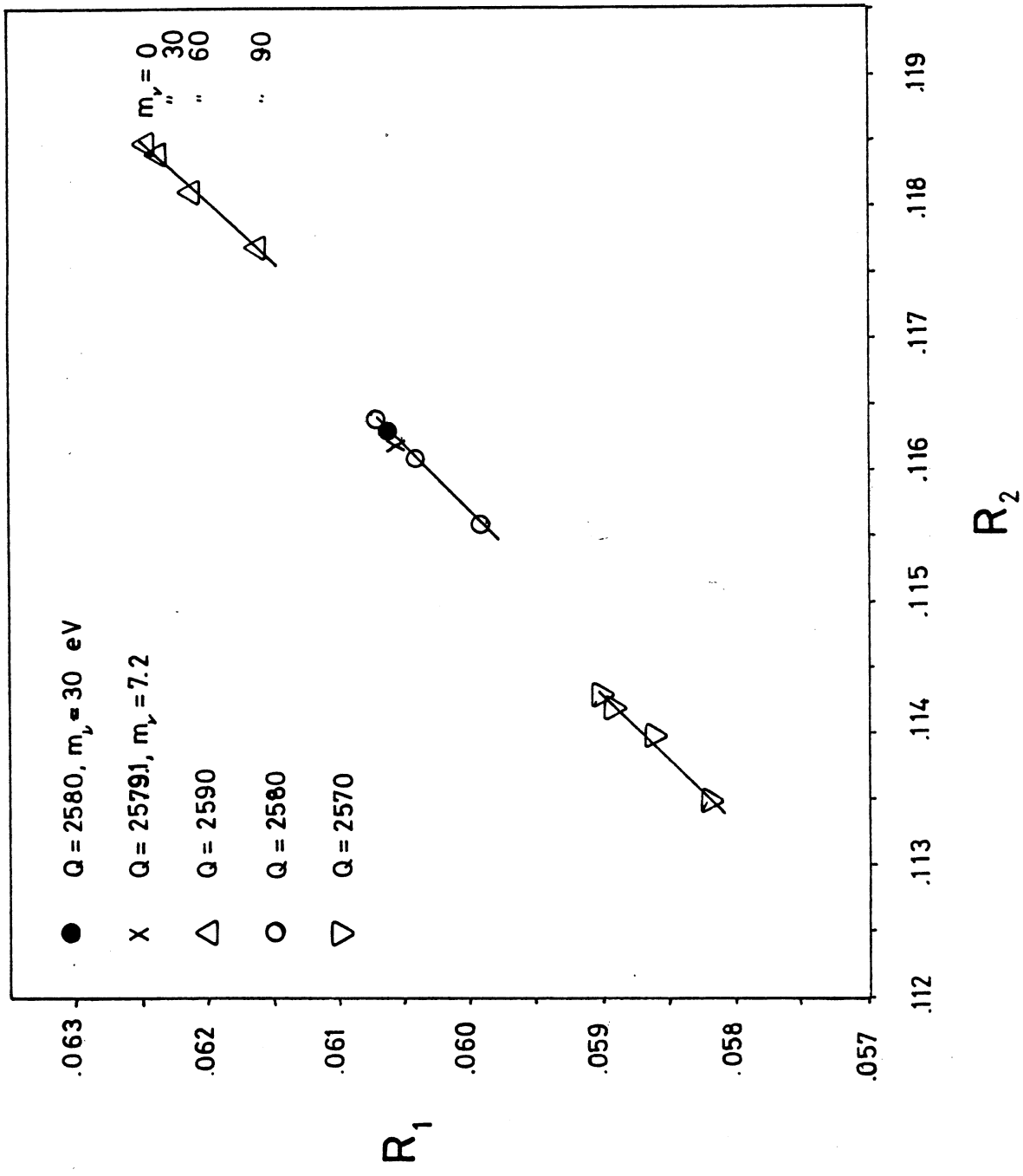
Q = 2580, m_ν = 30 eV
X Q = 2579.1, m_ν = 7.2
Q = 2590
Q = 2580
Q = 2570
m_ν = 0
" 30
" 60
" 90
.063
.062
.061
.060
.059
.058
.057
.112
.113
.114
.115
.116
.117
.118
.119
R_1
R_2

Fig. 2

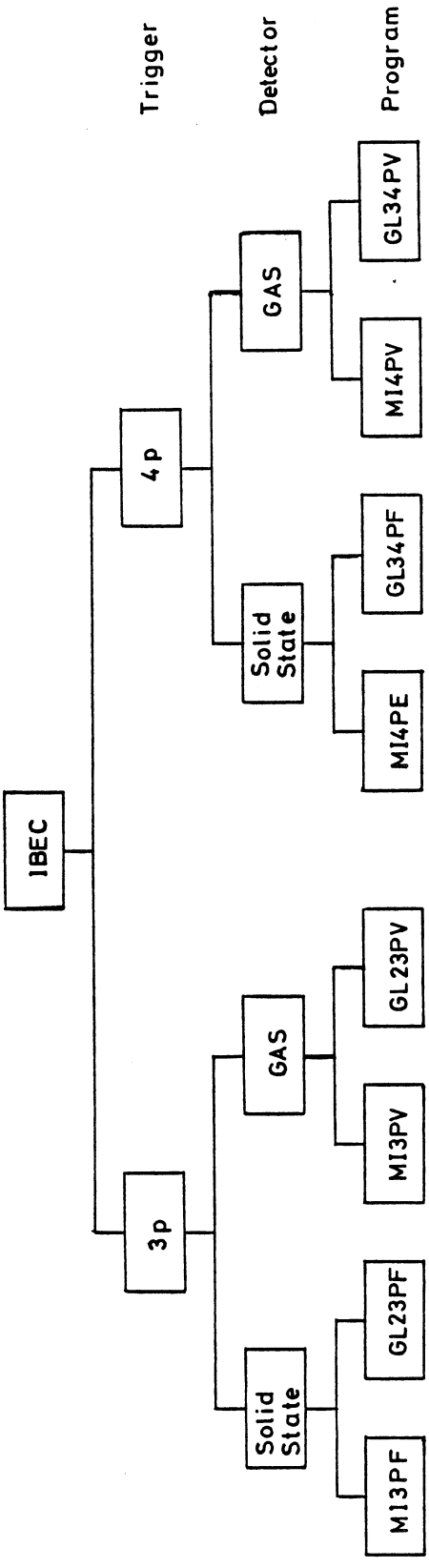
Trigger
Detector
Program
1BEC
4p
3p
GAS
Solid State
GAS
Solid State
GL34PV
M14PV
GL34PF
M14PE
GL23PV
M13PV
GL23PF
M13PF

Fig. 3

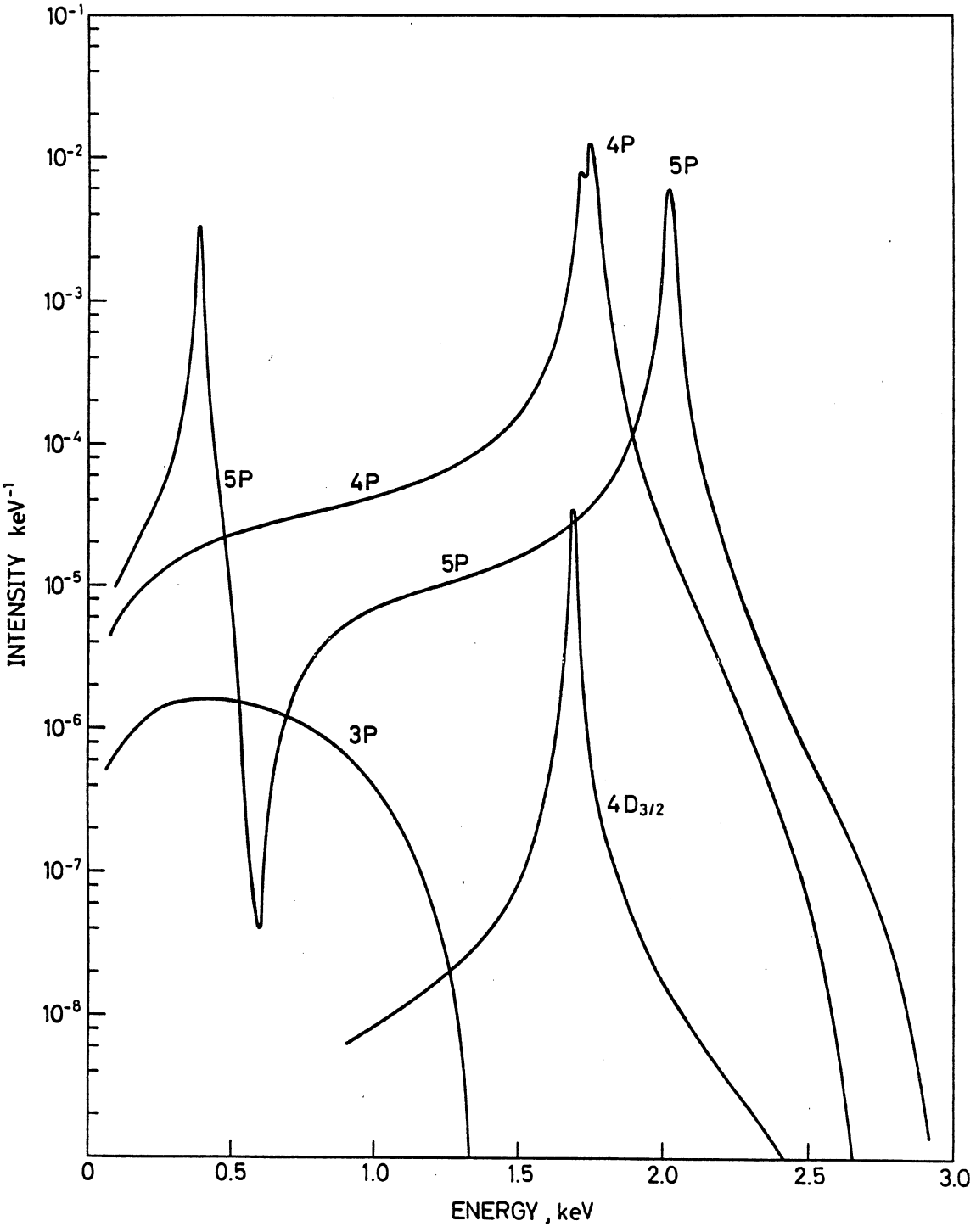
INTENSITY keV⁻¹
10⁻¹
10⁻²
10⁻³
10⁻⁴
10⁻⁵
10⁻⁶
10⁻⁷
10⁻⁸
0
0.5
1.0
1.5
2.0
2.5
3.0
ENERGY , keV
4P
5P
5P
4P
5P
3P
4D3/2

Fig. 4

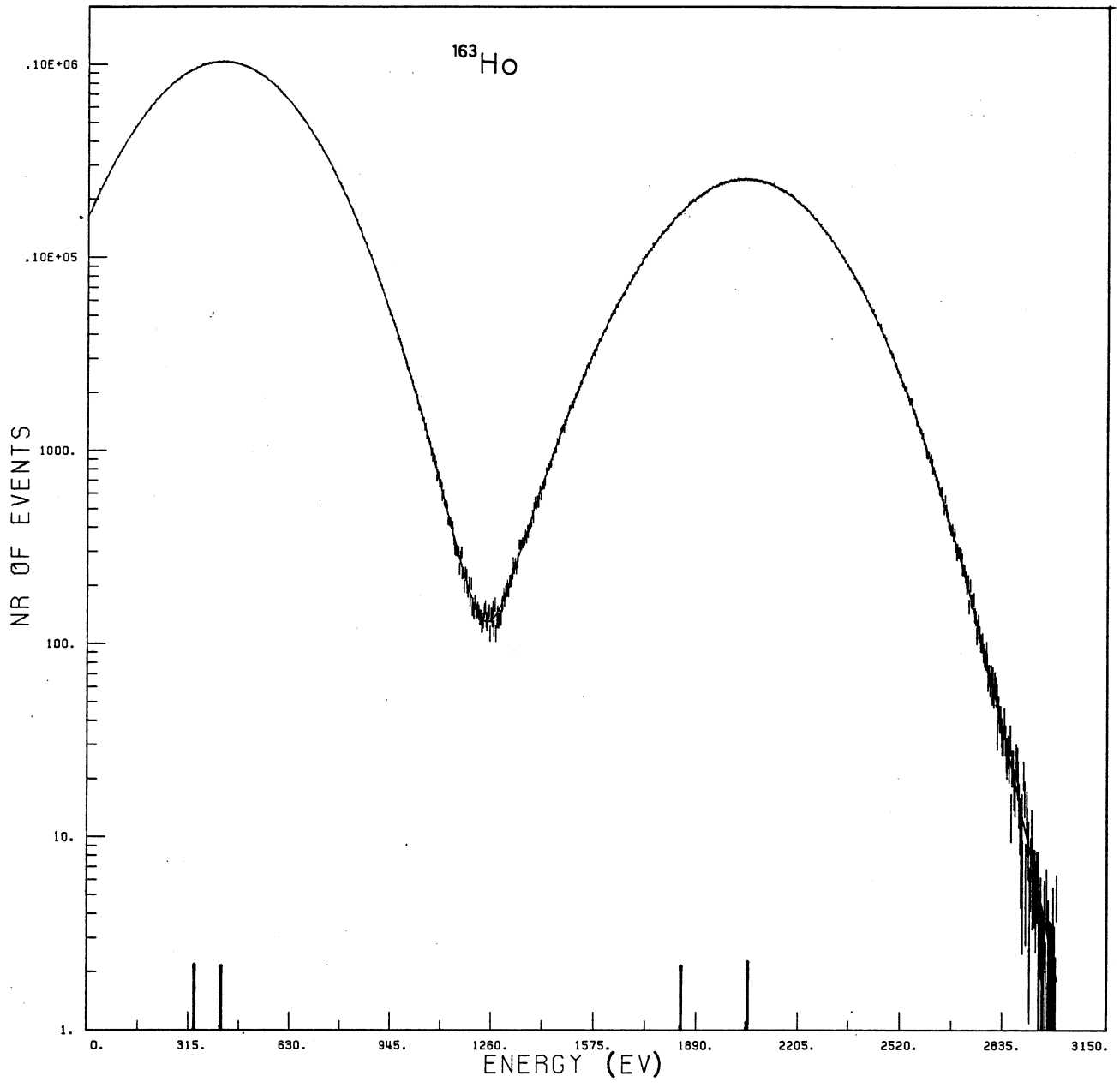
^{163}Ho
.10E+06
.10E+05
1000.
100.
10.
1.
NR OF EVENTS
0.
315.
630.
945.
1260.
1575.
1890.
2205.
2520.
2835.
3150.
ENERGY (EV)

Fig. 5

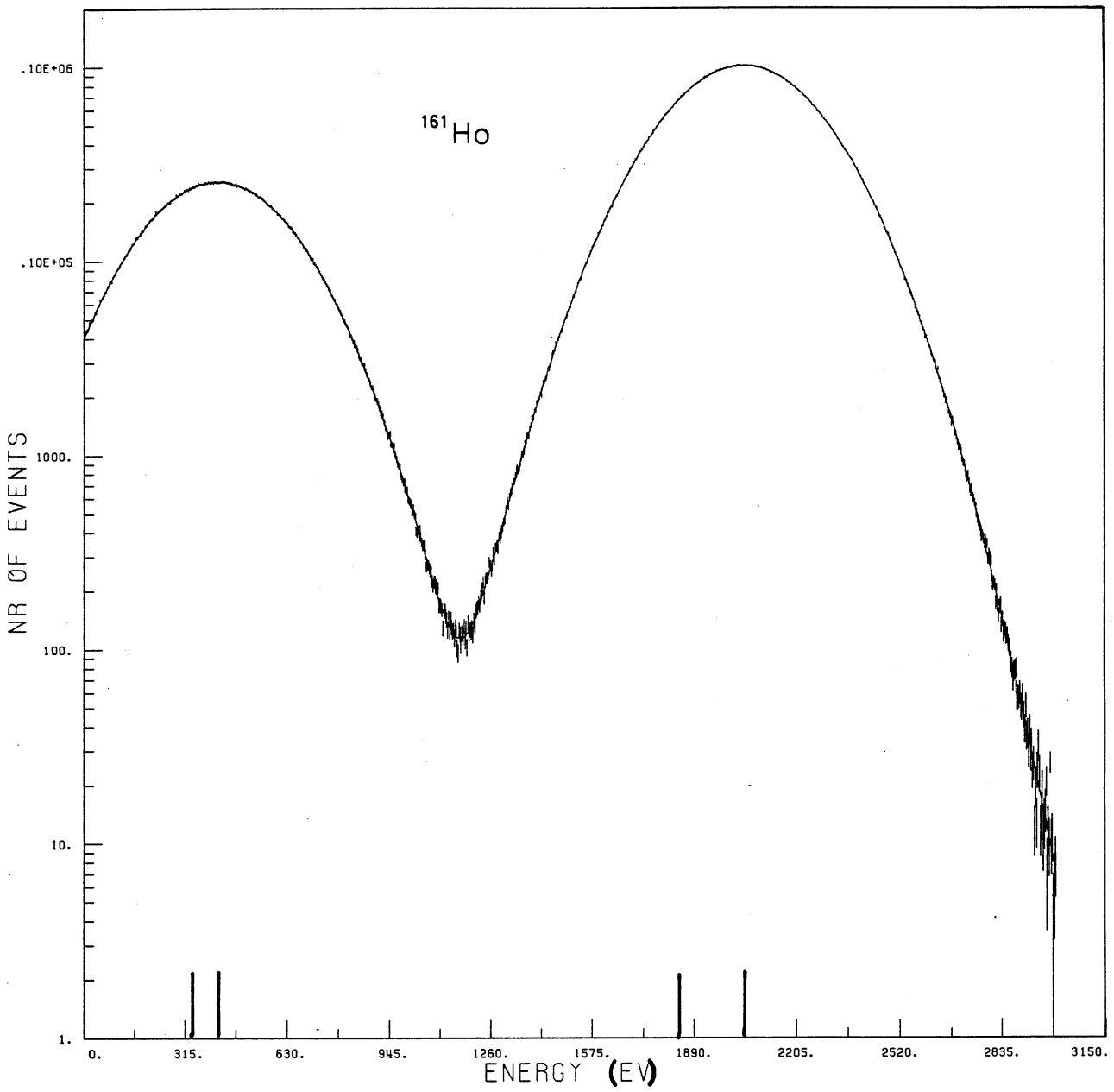
^{161}Ho
.10E+06
.10E+05
1000.
100.
10.
1.
NR ØF EVENTS
0.
315.
630.
945.
1260.
1575.
1890.
2205.
2520.
2835.
3150.
ENERGY (EV)

Fig. 6

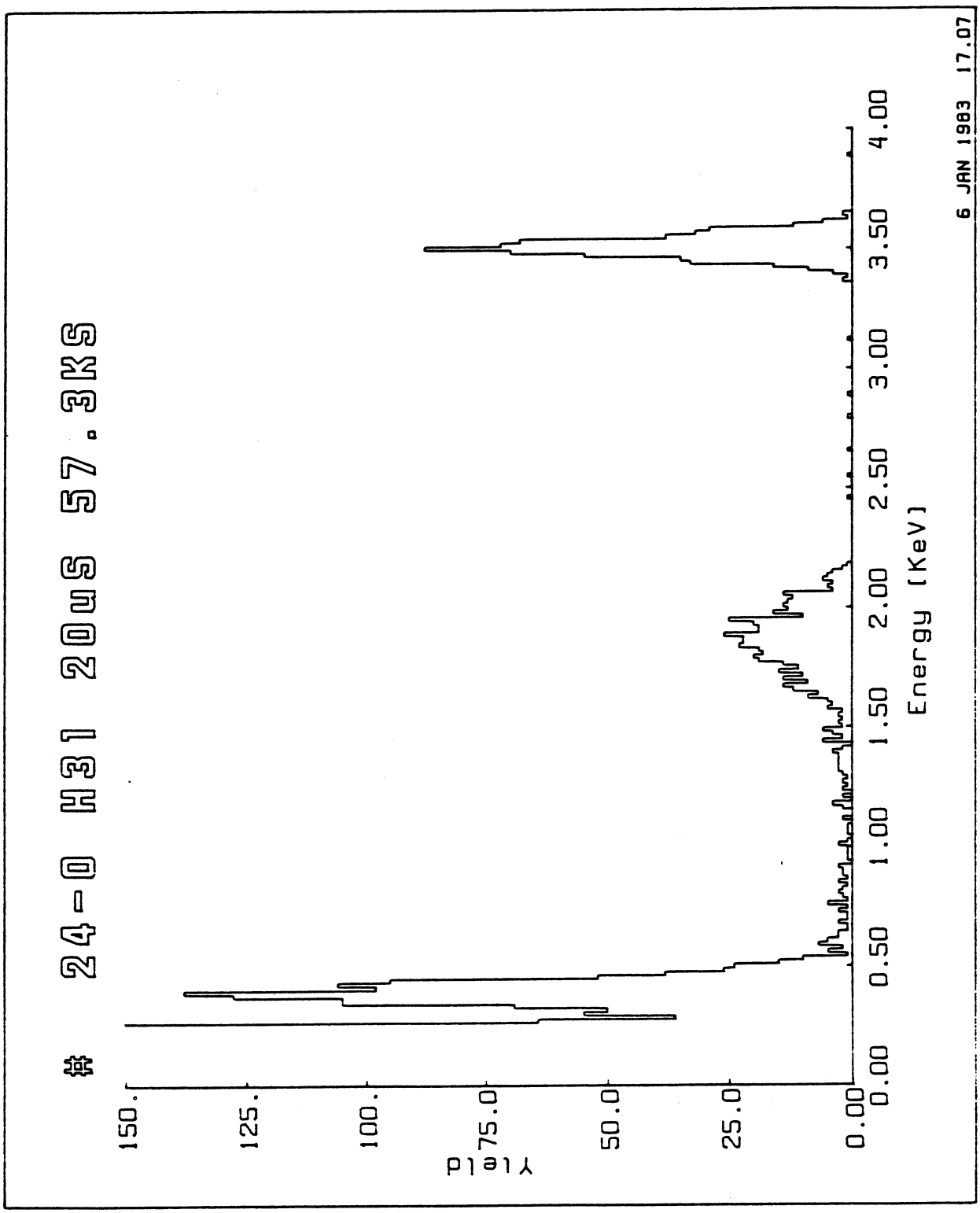
24-0 H31 20uS 57.3KS
6 JAN 1983 17.07
Yield
150.
125.
100.
75.0
50.0
25.0
0.00
0.00
0.50
1.00
1.50
2.00
2.50
3.00
3.50
4.00
Energy [KeV]

Fig. 7

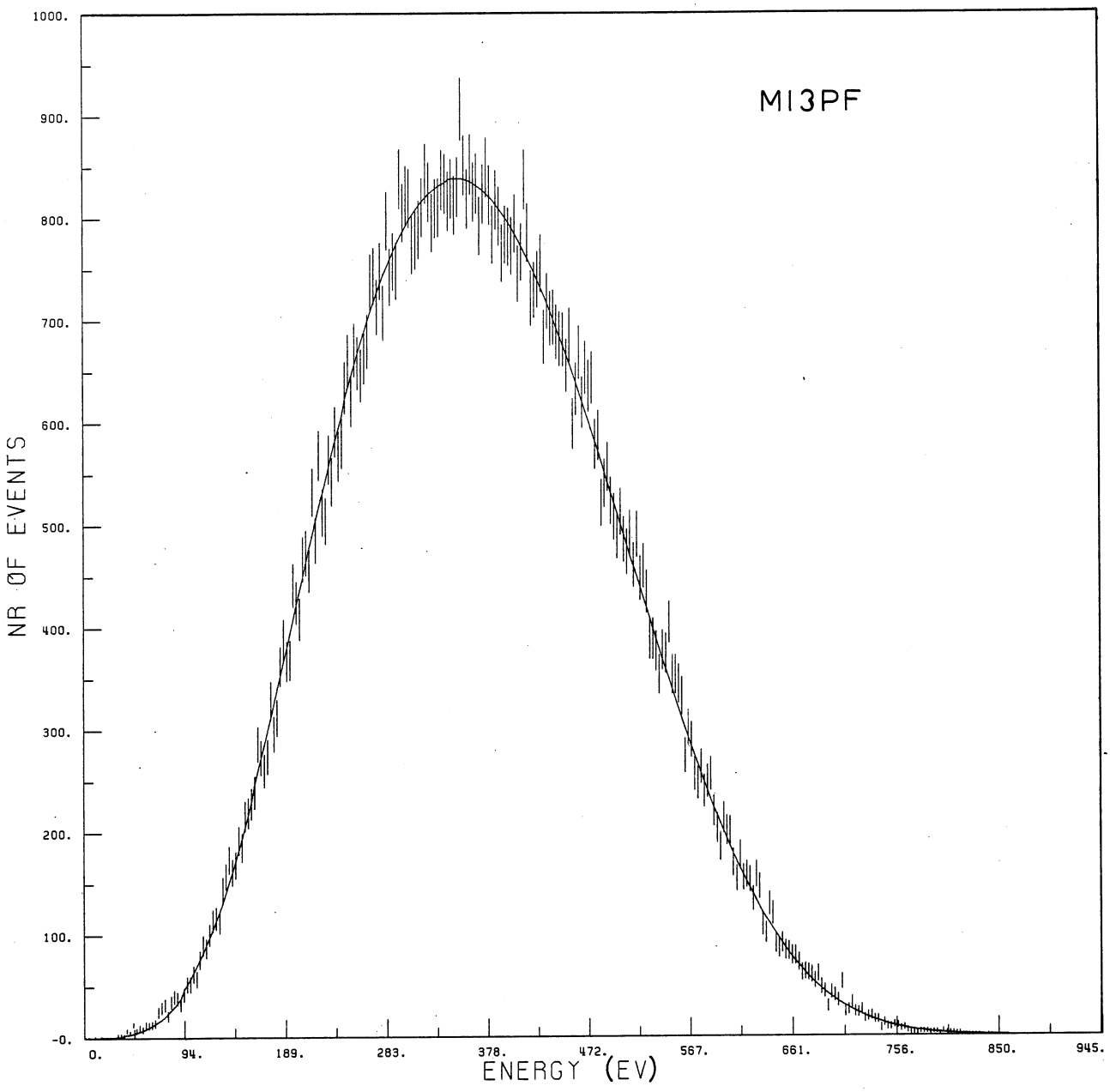
M13PF
NR OF EVENTS
ENERGY (EV)
1000.
900.
800.
700.
600.
500.
400.
300.
200.
100.
-0.
0.
94.
189.
283.
378.
472.
567.
661.
756.
850.
945.

Fig. 8

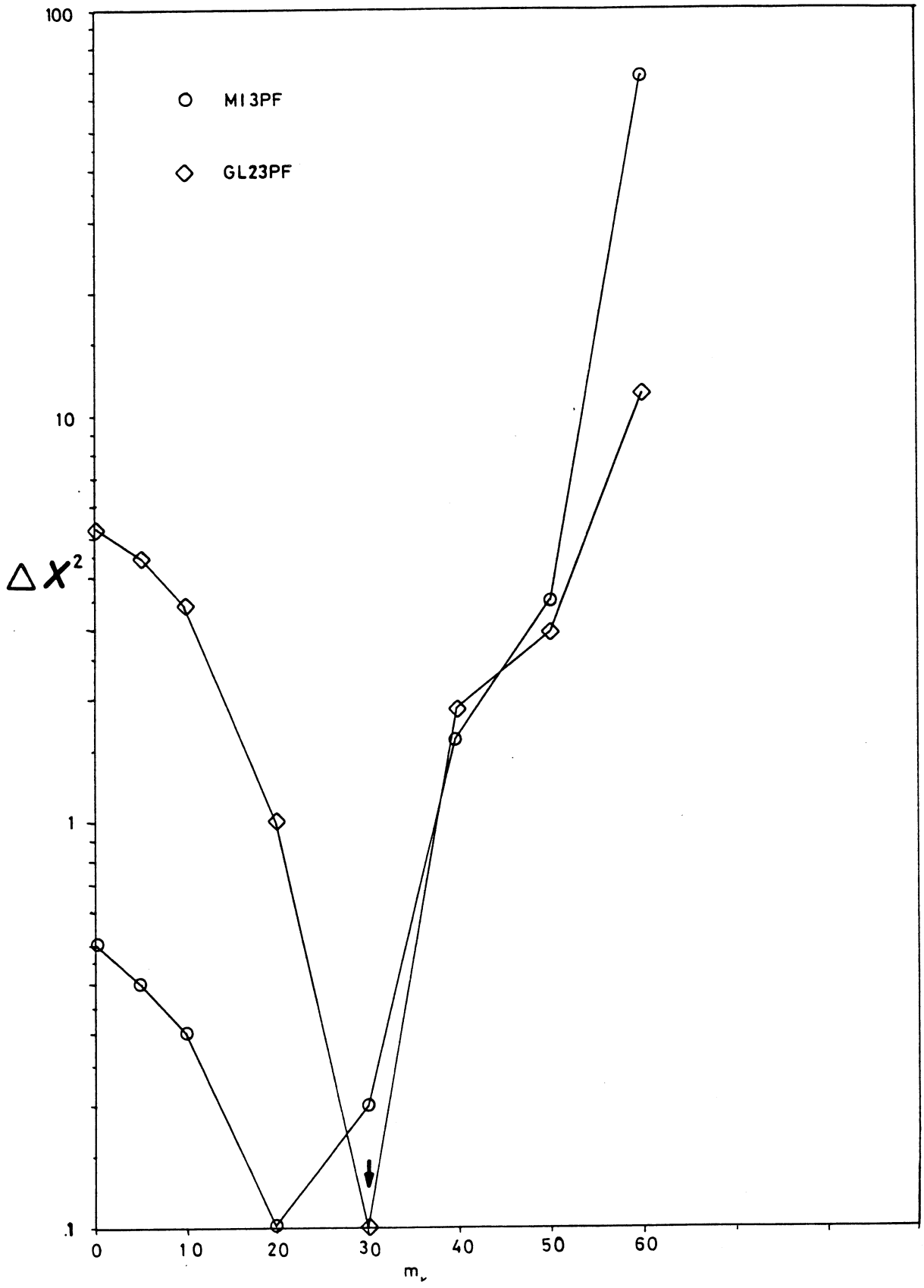

Fig. 9

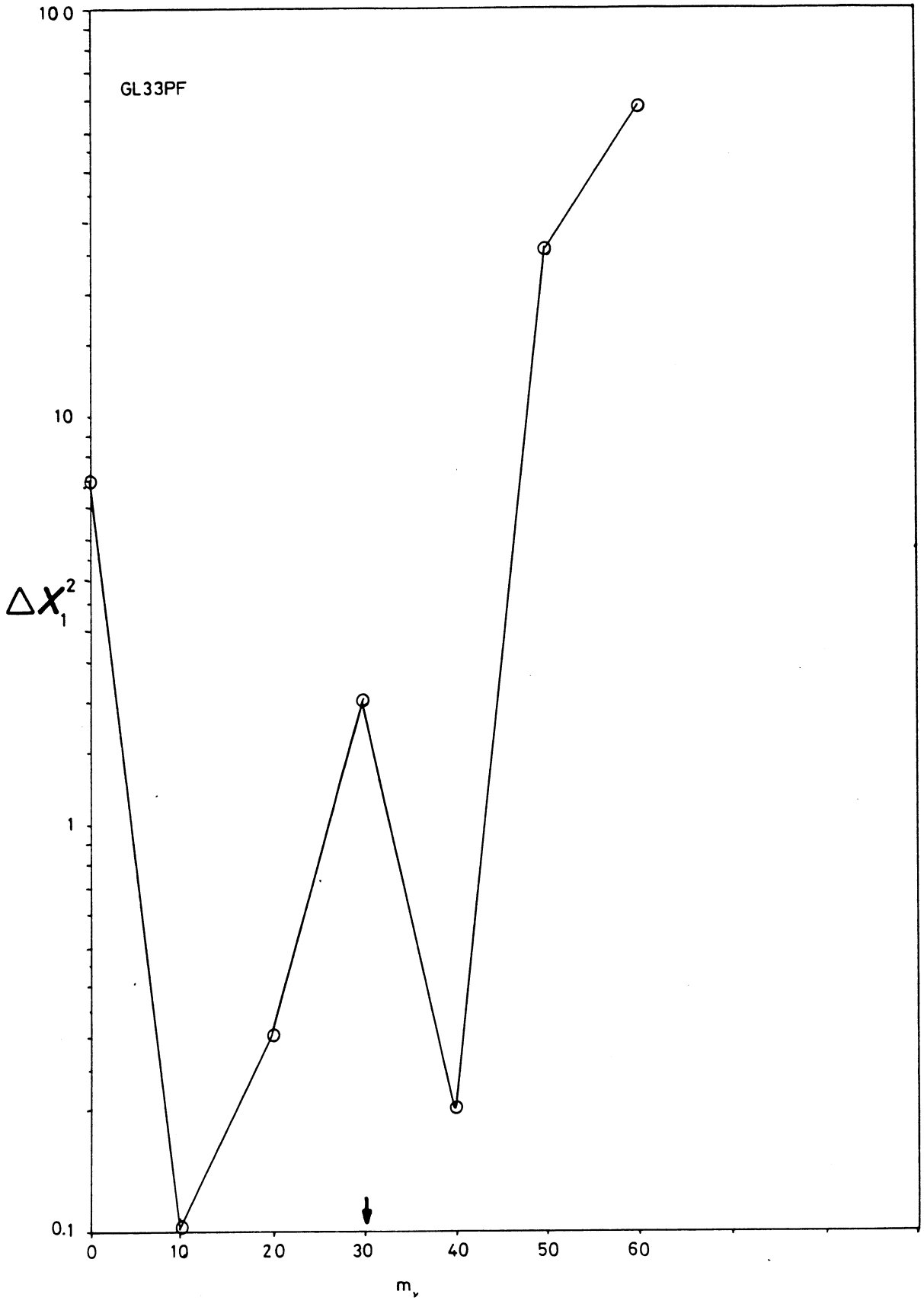

Fig. 10

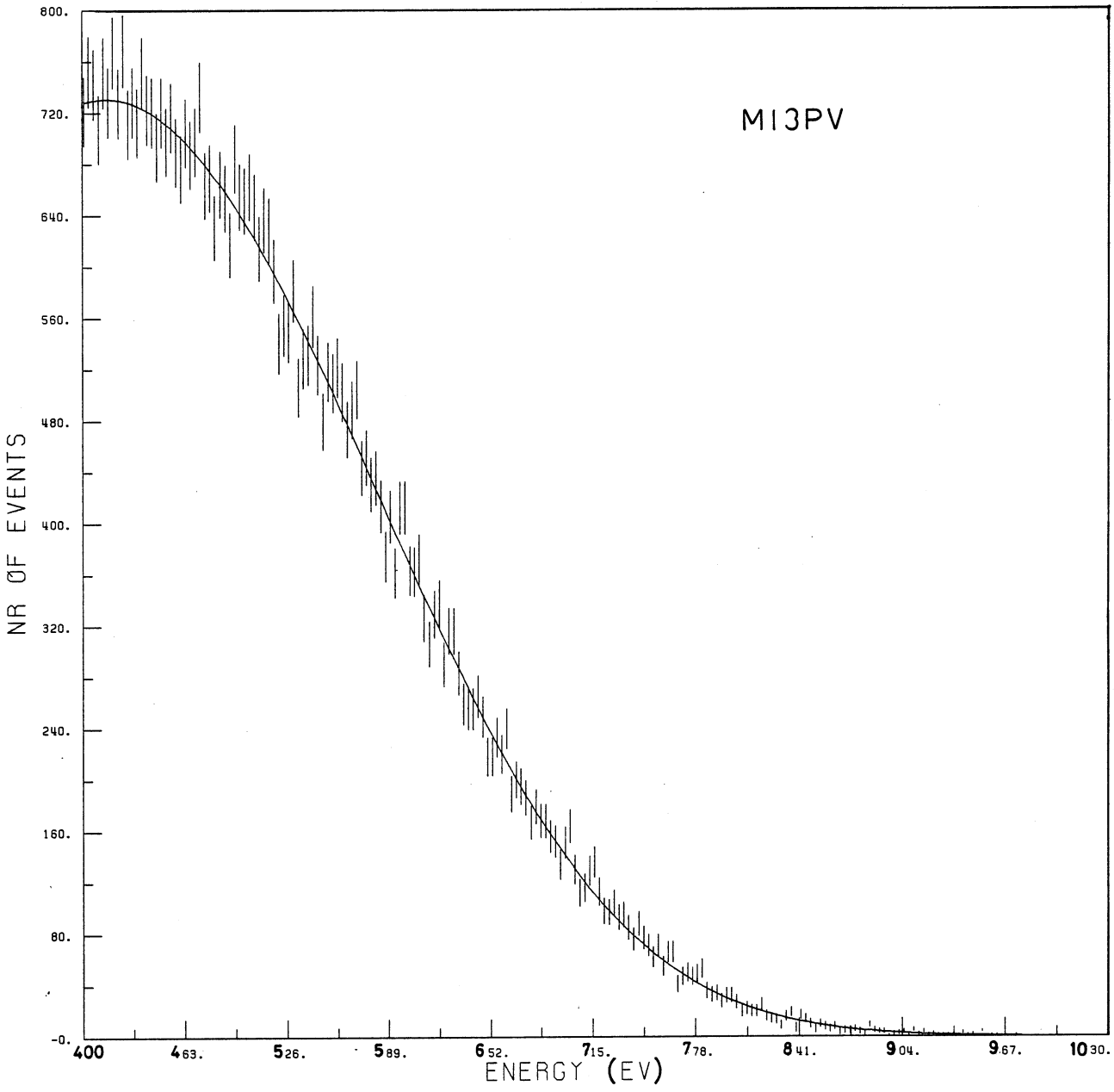
M13PV
NR OF EVENTS
800.
720.
640.
560.
480.
400.
320.
240.
160.
80.
-0.
400
463.
526.
589.
652.
715.
778.
841.
904.
967.
1030.
ENERGY (EV)

Fig. 11

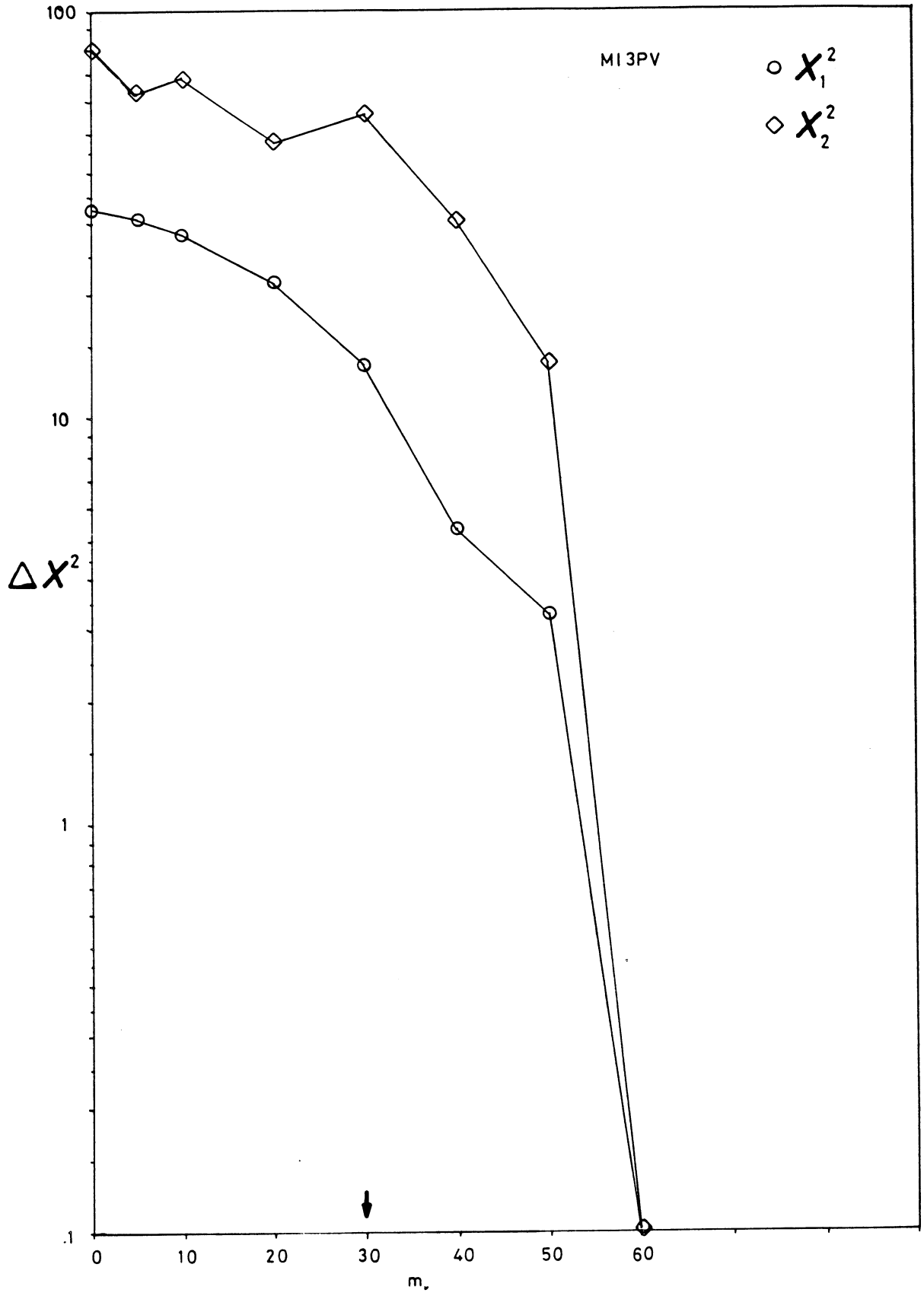

Fig. 12

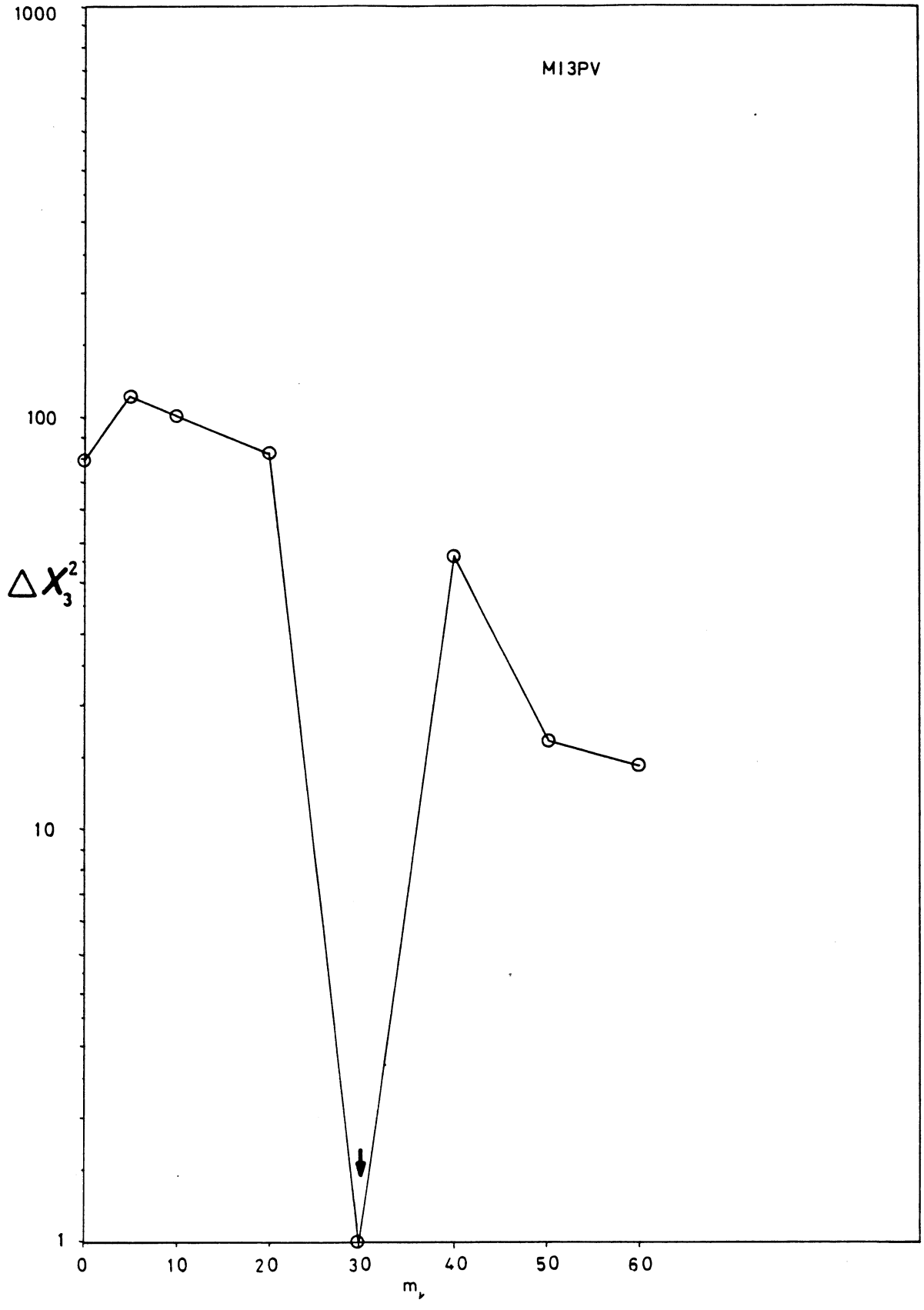

Fig. 13

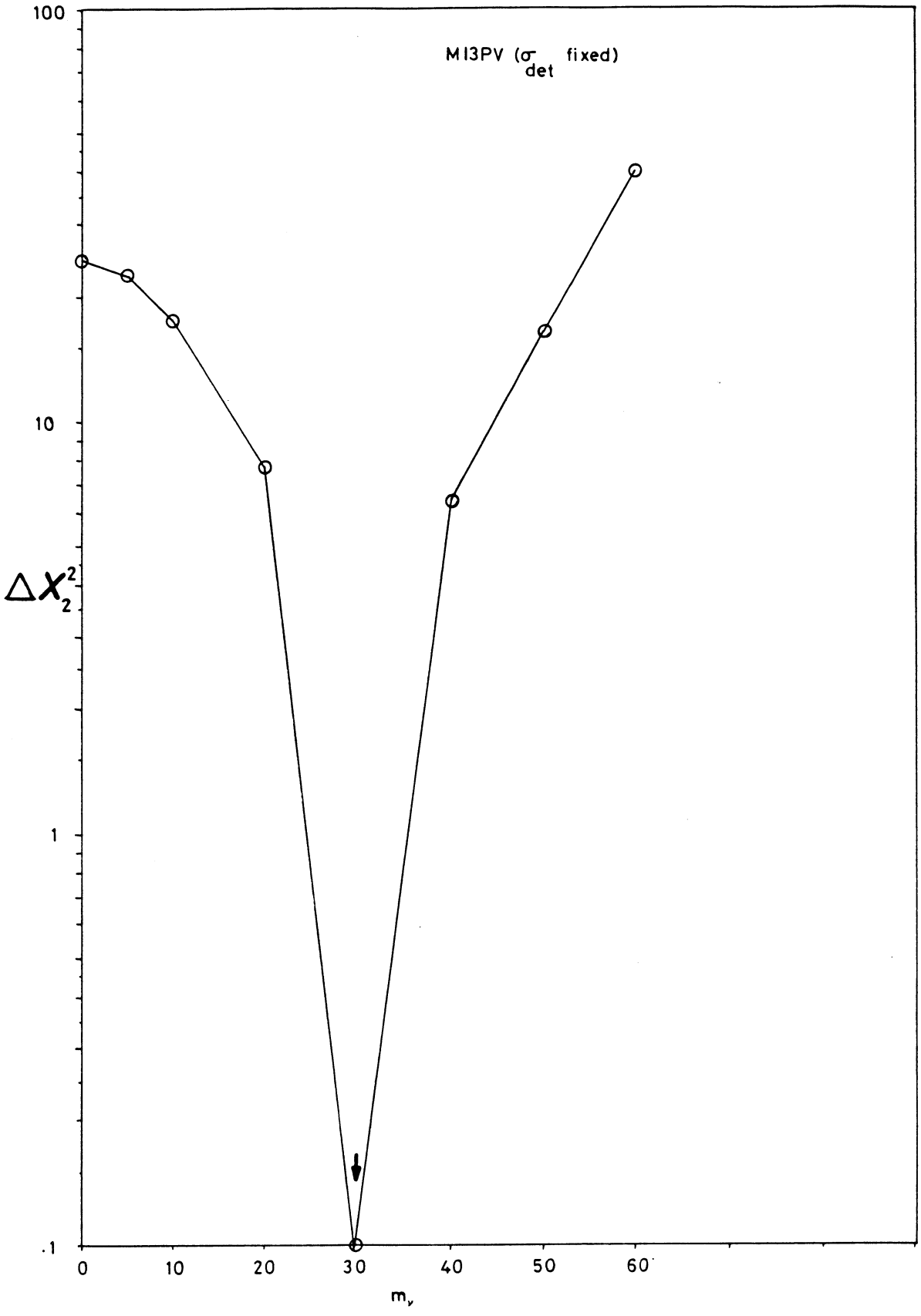
MI3PV (σ_{det} fixed)
100
10
1
.1
$\Delta\chi^2_2$
0
10
20
30
40
50
60
m_ν

Fig. 14

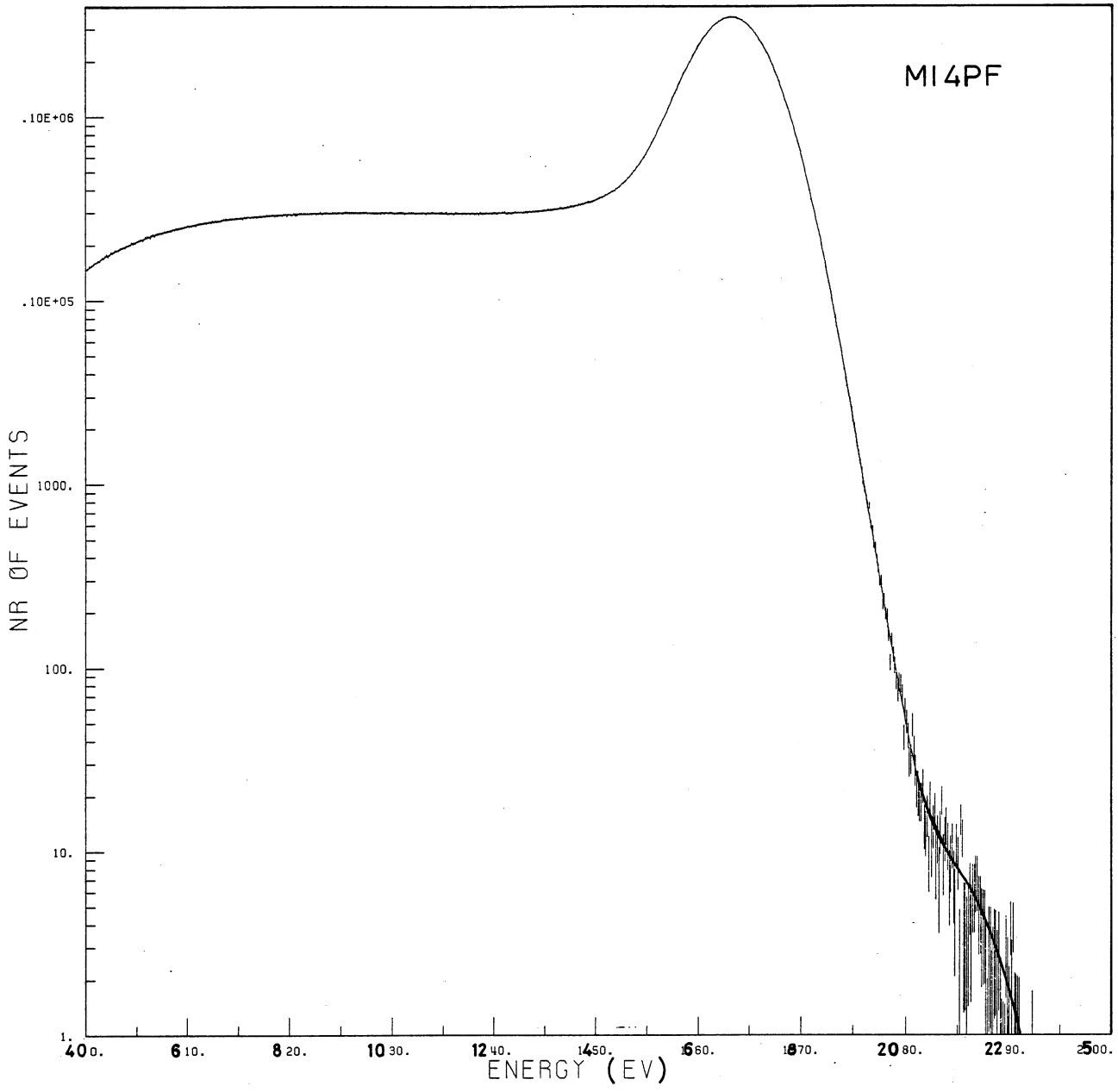
M14PF
.10E+06
.10E+05
1000.
100.
10.
1.
NR ØF EVENTS
400.
610.
820.
1030.
1240.
1450.
1660.
1870.
2080.
2290.
2500.
ENERGY (EV)

Fig. 15

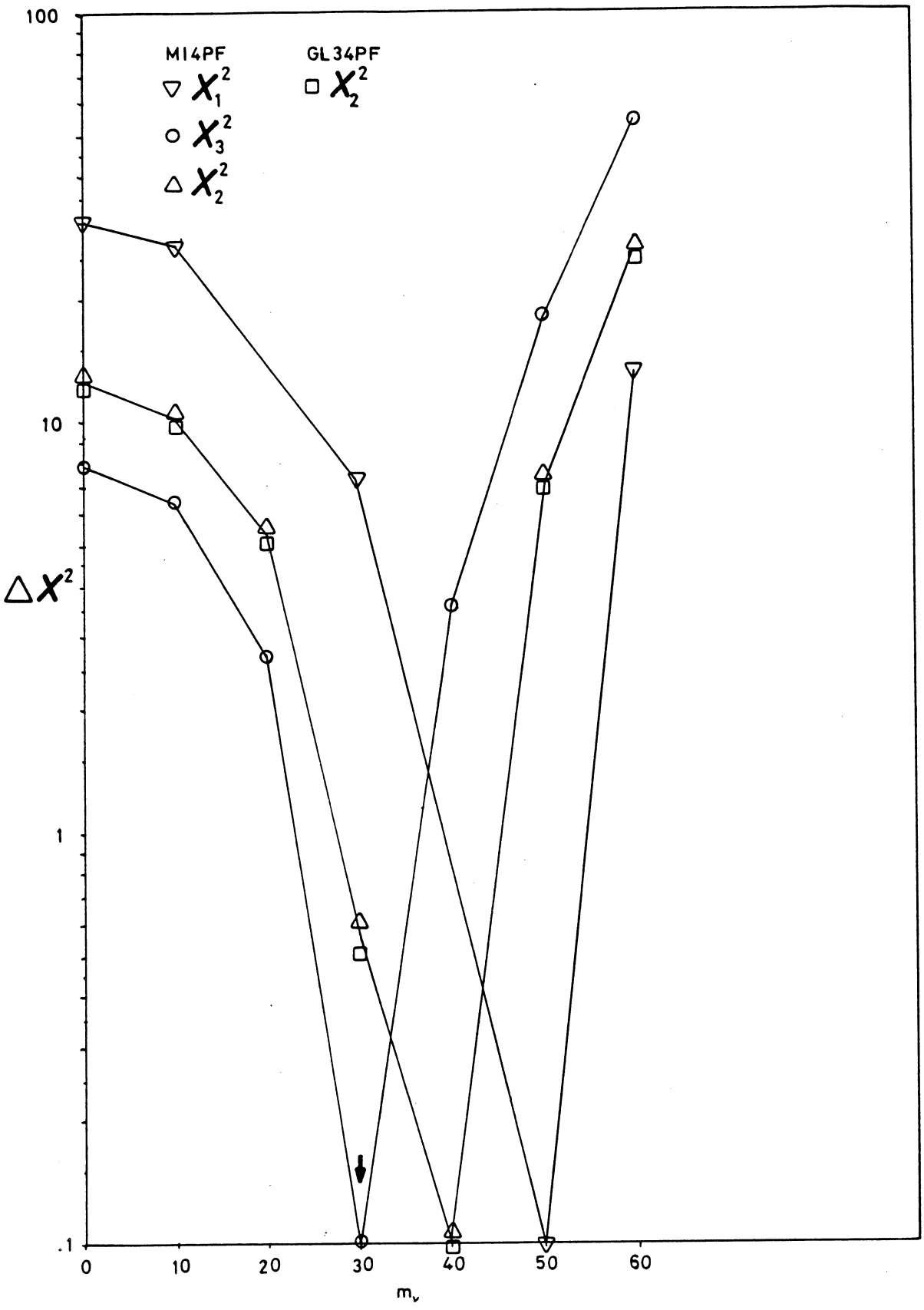
100
10
1
.1
MI4PF
GL34PF
∇X_1^2
$\square X_2^2$
$\circ X_3^2$
$\triangle X_2^2$
ΔX^2
0
10
20
30
40
50
60
m_ν

Fig. 16

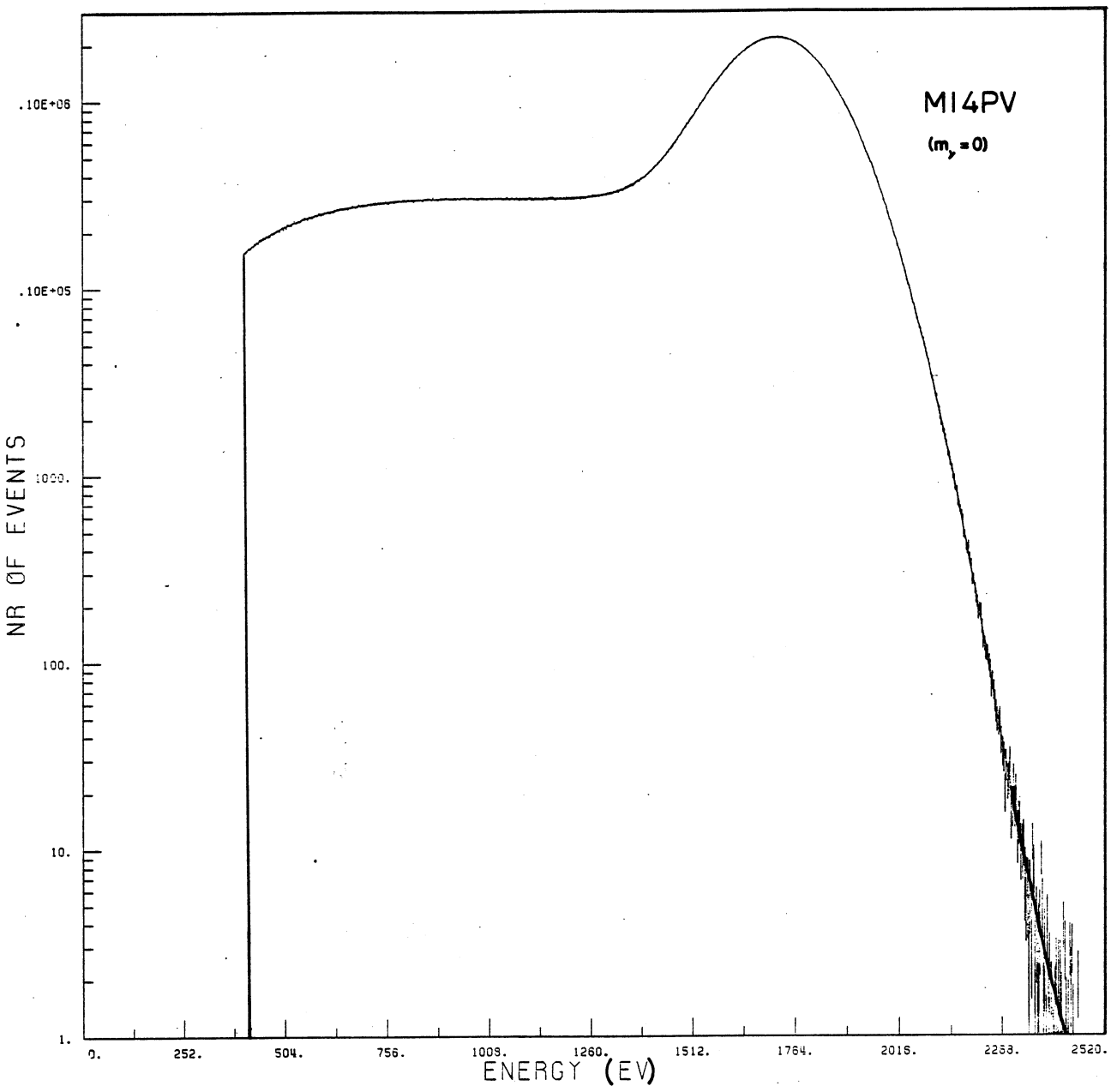
M14PV
($m_\gamma = 0$)
.10E+06
.10E+05
1000.
100.
10.
1.
NR OF EVENTS
0.
252.
504.
756.
1008.
1260.
1512.
1764.
2016.
2268.
2520.
ENERGY (EV)

Fig. 17

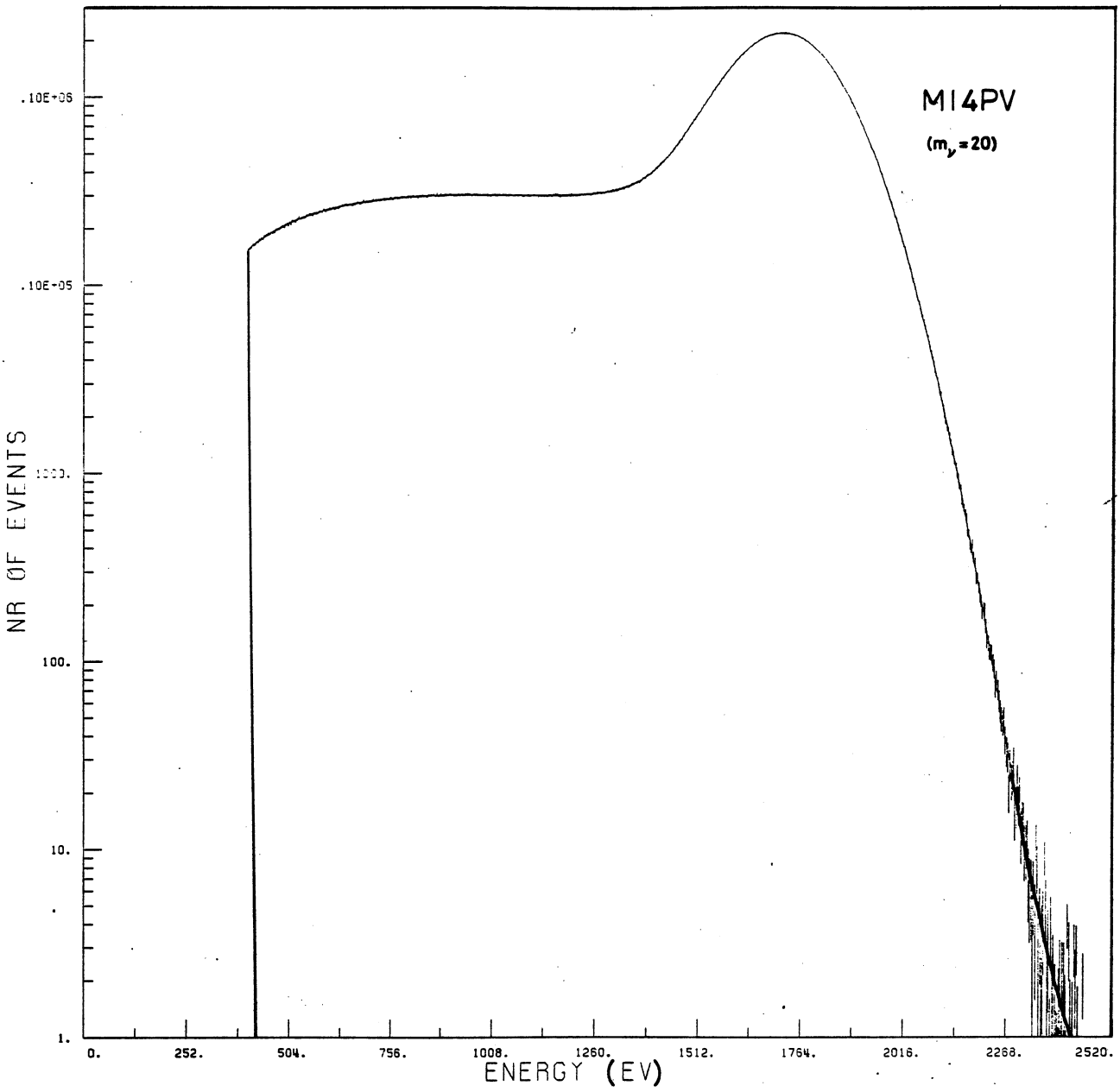
M14PV
(m_ν=20)
.10E+06
.10E-05
1000.
100.
10.
1.
NR OF EVENTS
0.
252.
504.
756.
1008.
1260.
1512.
1764.
2016.
2268.
2520.
ENERGY (EV)

Fig. 18

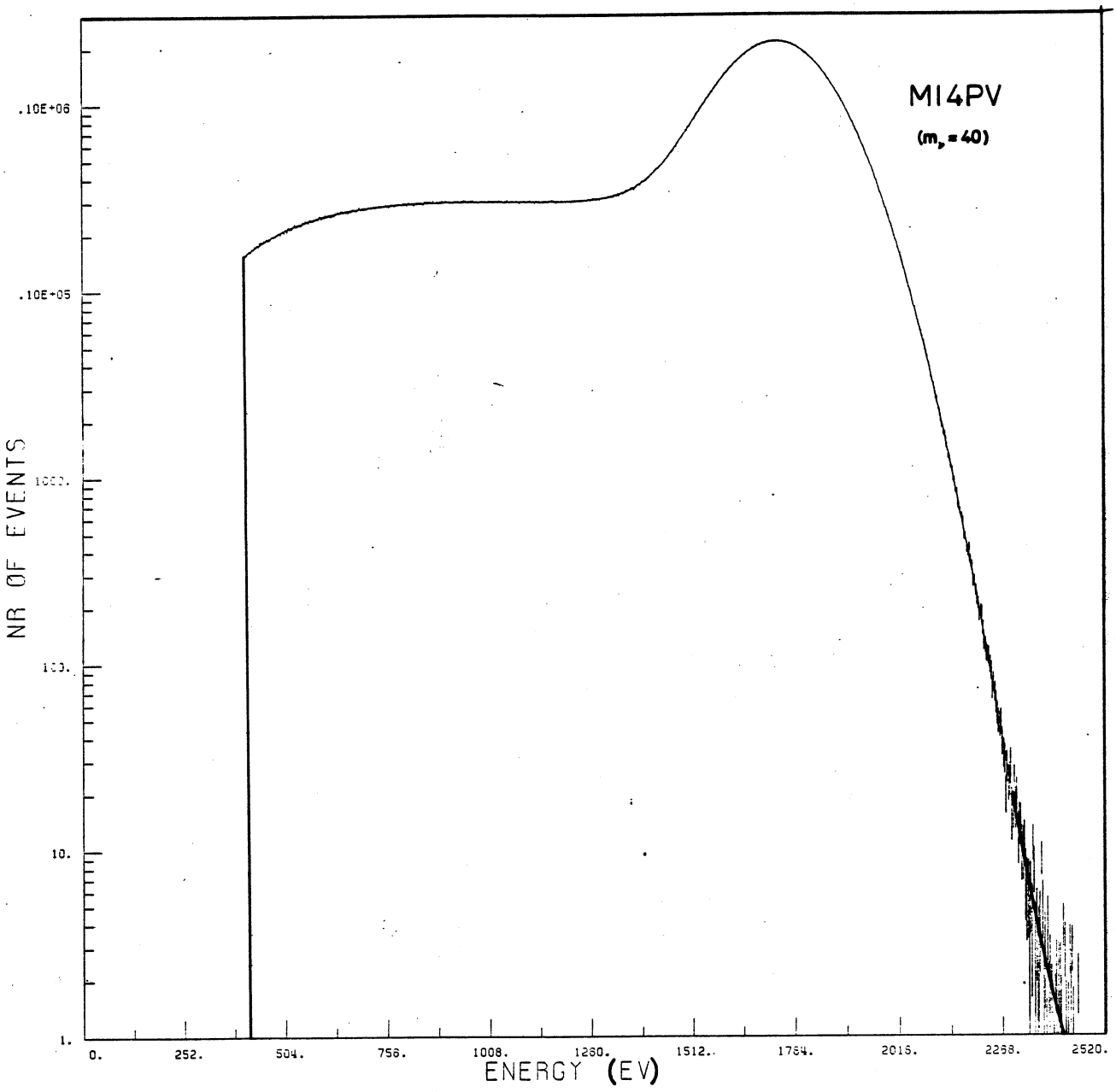
M14PV
(m$_p$=40)
.10E+06
.10E+05
1000.
100.
10.
1.
NR OF EVENTS
0.
252.
504.
756.
1008.
1260.
1512.
1764.
2016.
2268.
2520.
ENERGY (EV)

Fig. 19

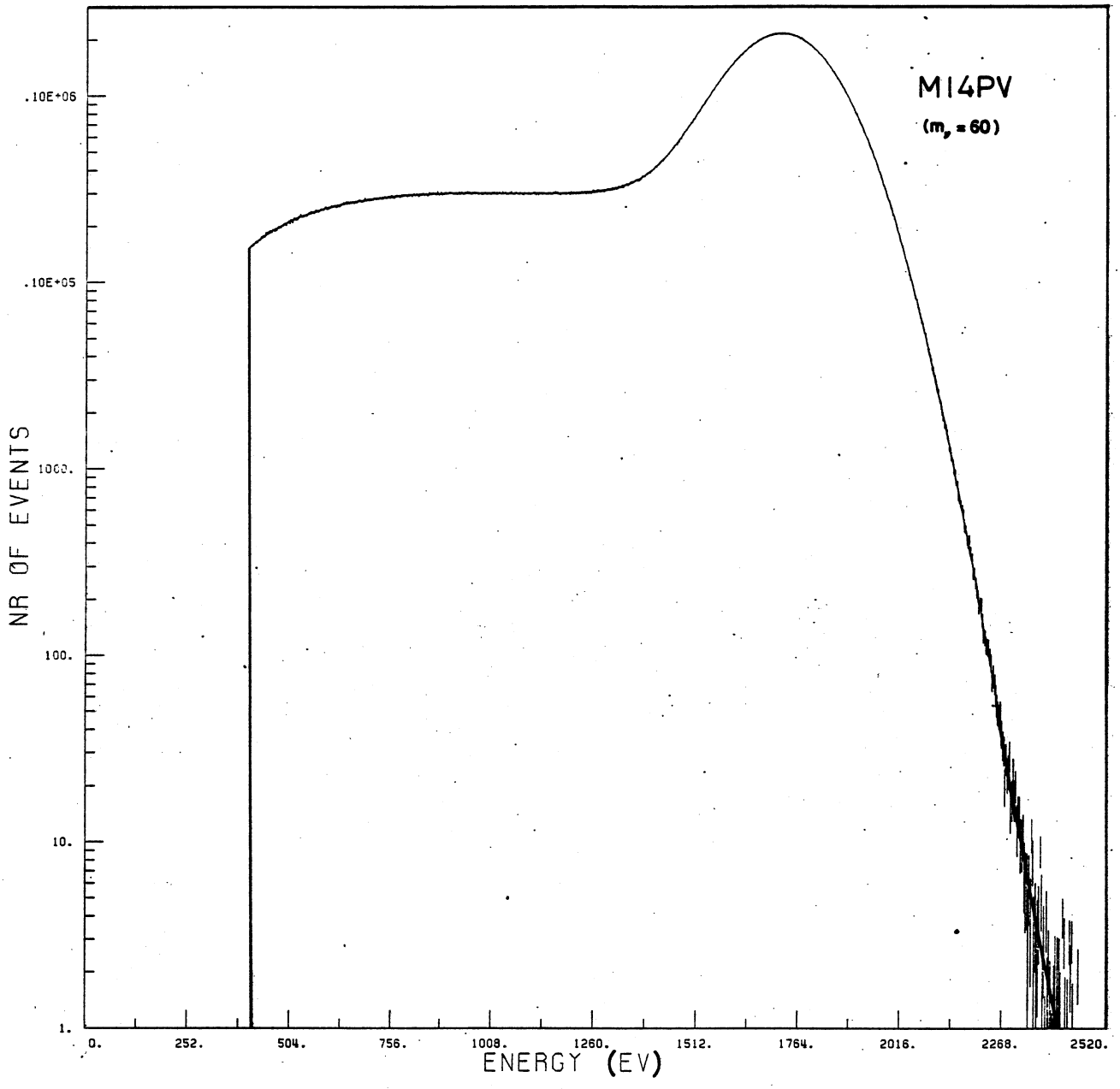
M14PV
(m_p = 60)
.10E+06
.10E+05
1000.
100.
10.
1.
NR OF EVENTS
0.
252.
504.
756.
1008.
1260.
1512.
1764.
2016.
2268.
2520.
ENERGY (EV)

Fig. 20

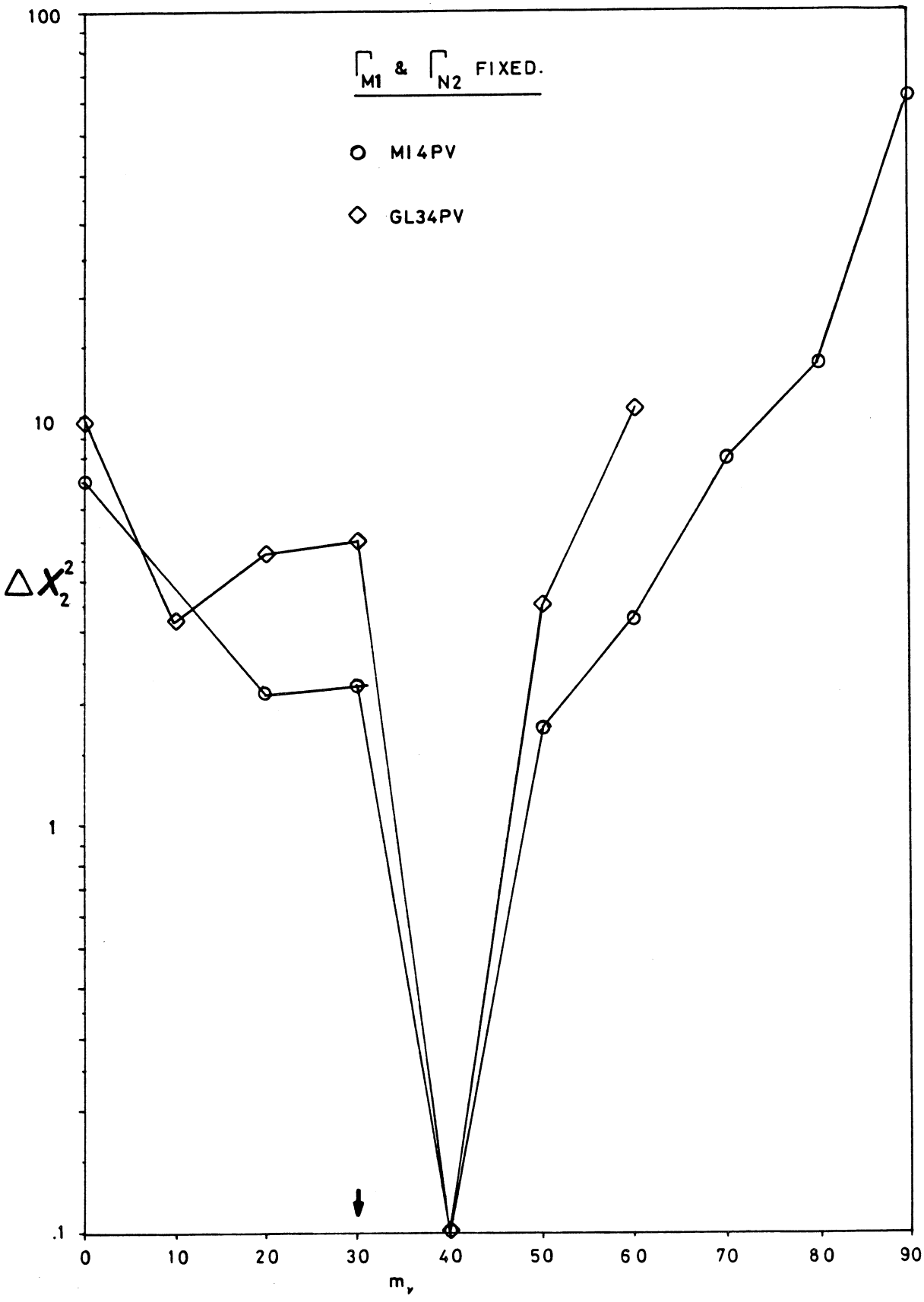
100
10
1
.1
Γ_{M1} & Γ_{N2} FIXED.
MI4PV
GL34PV
ΔX_2^2
0
10
20
30
40
50
60
70
80
90
m_ν

Fig. 21

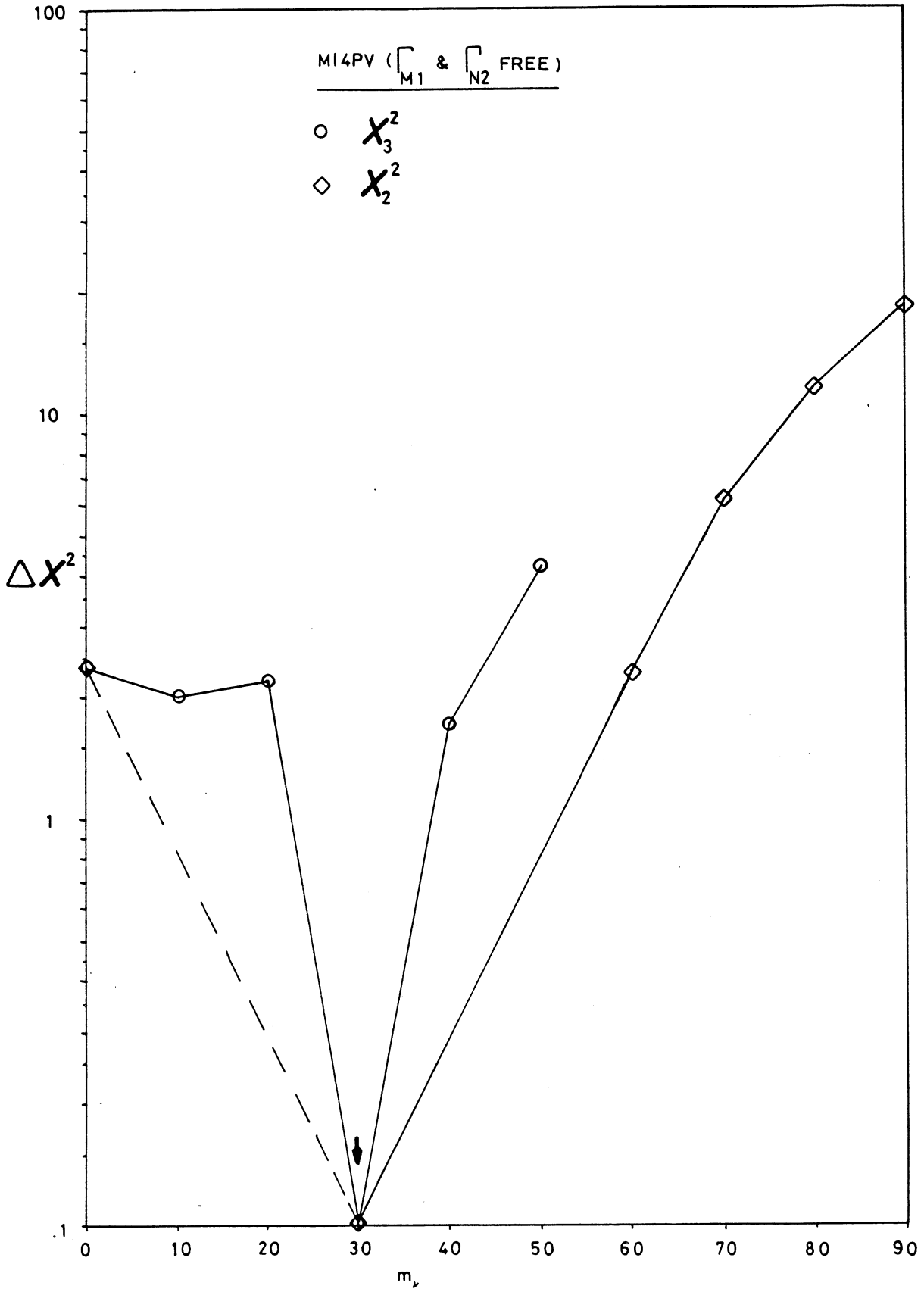
MI4PV (Γ M1 & Γ N2 FREE)
χ_3^2
χ_2^2
$\Delta\chi^2$
100
10
1
.1
0
10
20
30
40
50
60
70
80
90
m_ν

Fig. 22

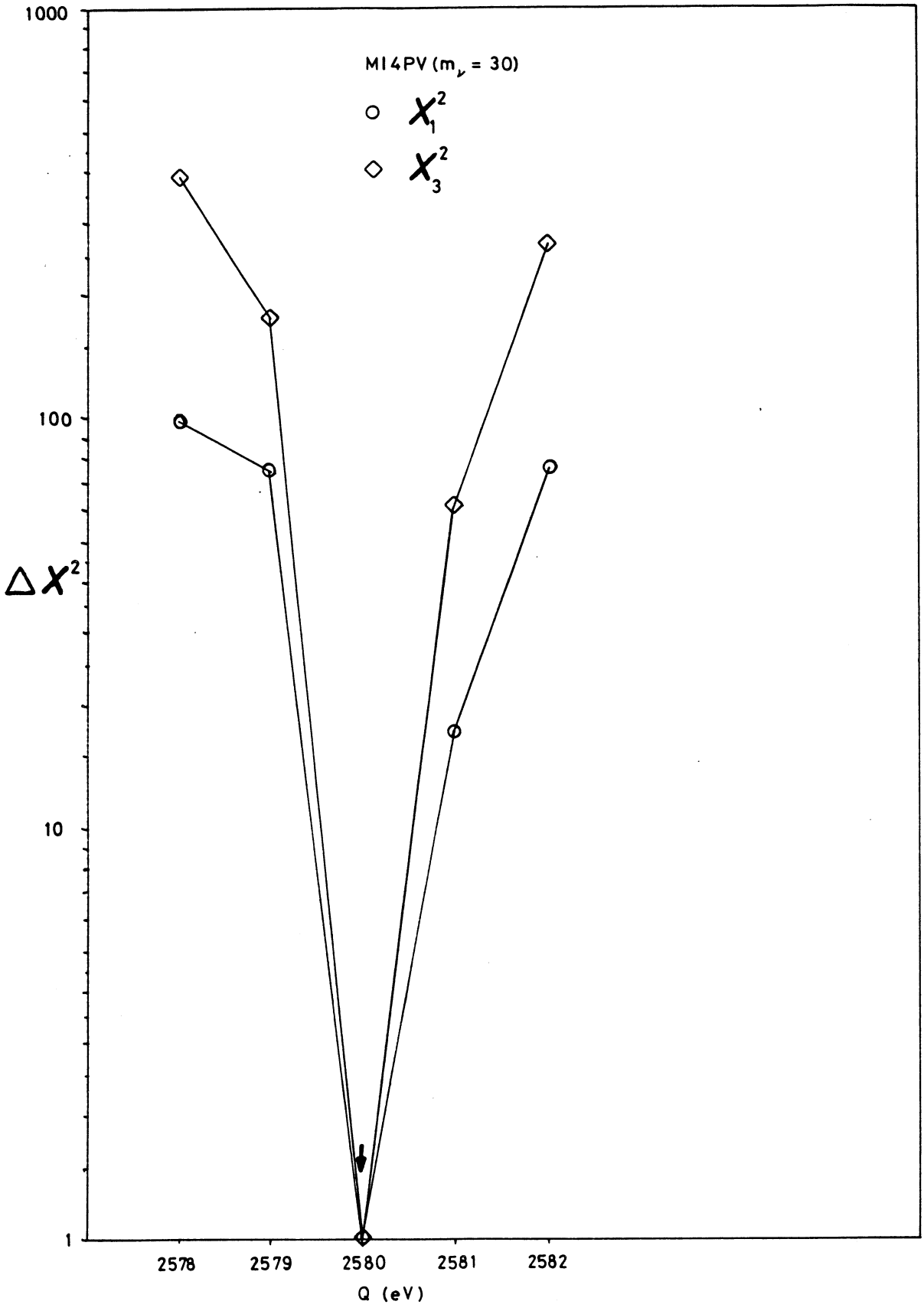
1000
100
10
1
M14PV (m_ν = 30)
χ_1^2
χ_3^2
$\Delta\chi^2$
2578
2579
2580
2581
2582
Q (eV)

Fig. 23

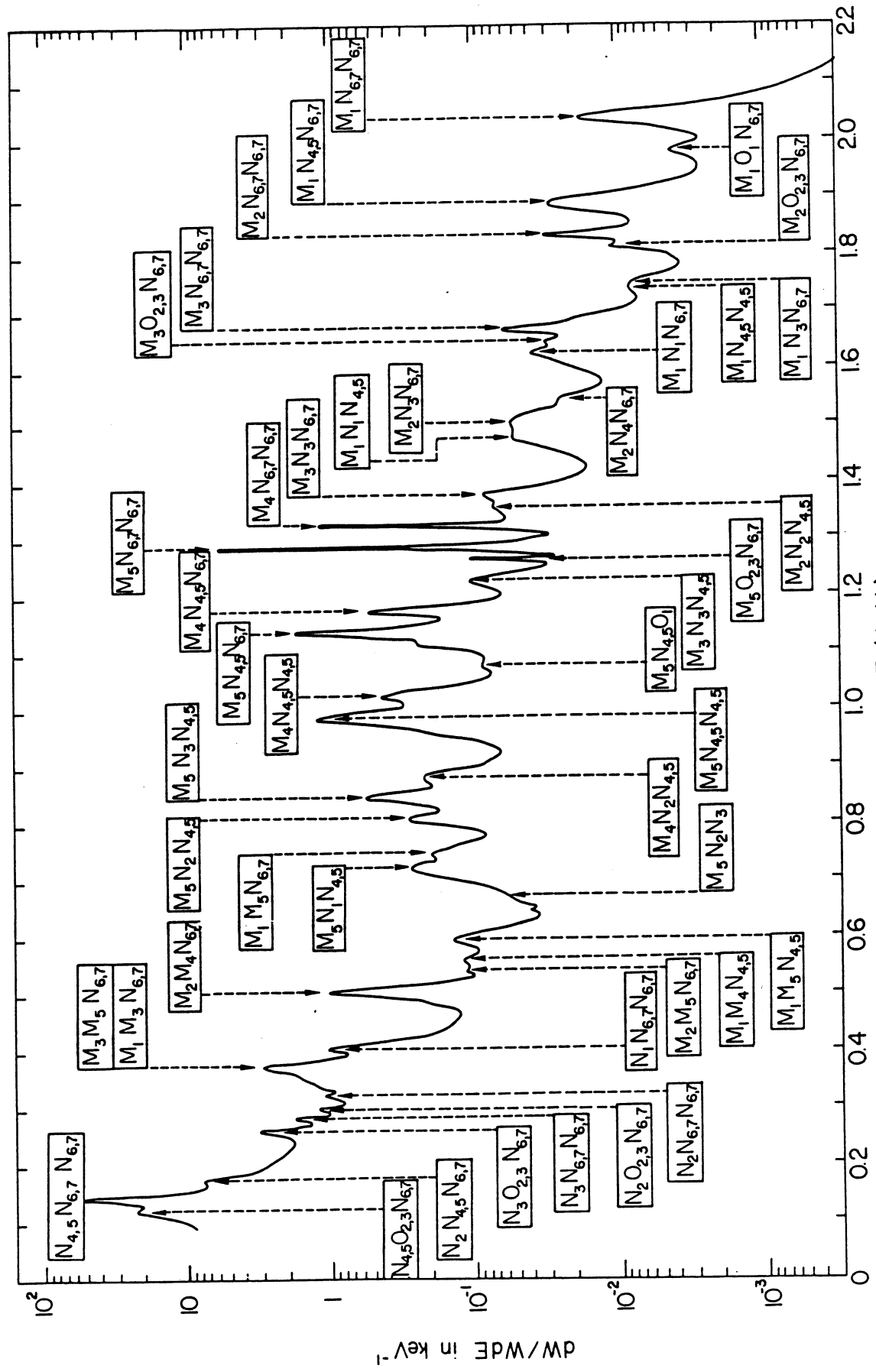
dW/WdE in keV⁻¹
E (keV)
N4,5 N6,7 N6,7
N4,5O2,3N6,7
N2 N4,5N6,7
N3O2,3 N6,7
N3N6,7N6,7
N2O2,3 N6,7
N2N6,7N6,7
M3M5 N6,7
M1 M3 N6,7
M2M4N6,7
M5N2N4,5
M1M5N6,7
M5N1N4,5
M5 N3N4,5
M4N4,5N6,7
M5N4,5N6,7
M4N4,5N4,5
M5N6,7N6,7
M4N4,5N6,7
M3O2,3N6,7
M3N6,7N6,7
M2N6,7N6,7
M1N4,5N6,7
M1N6,7N6,7
M4N6,7N6,7
M3N3N6,7
M1N1N4,5
M2N3N6,7
M2N4N6,7
N1N6,7N6,7
M2M5N6,7
M1M4N4,5
M1M5N4,5
M4N2N4,5
M5N4,5N4,5
M5N2N3
M5O2,3N6,7
M2N2N4,5
M5N4,5O1
M3N3N4,5
M1N1N6,7
M1N45N4,5
M1N3N6,7
M1O1N6,7
M2O2,3N6,7

Fig. 24

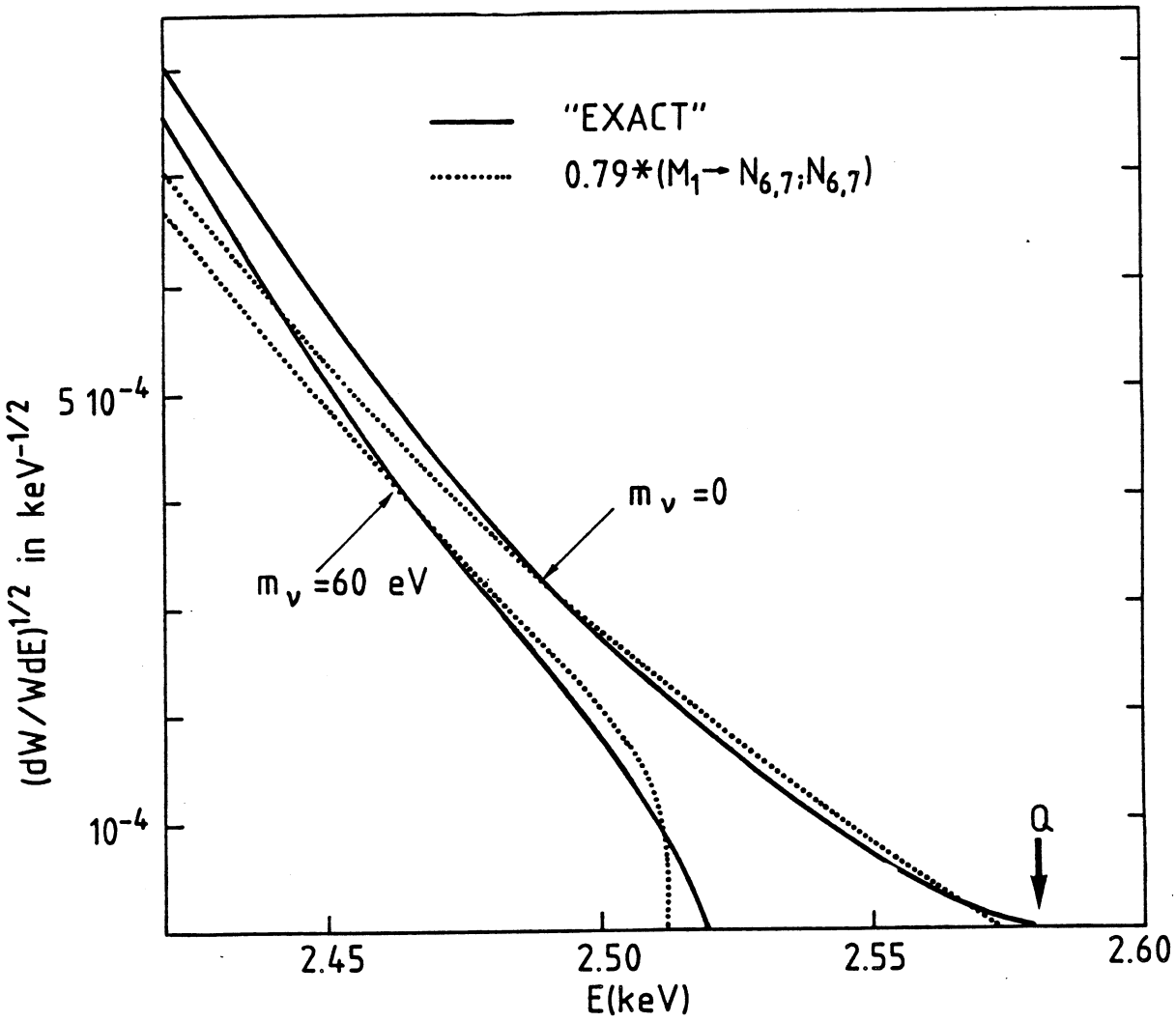
"EXACT"
0.79*(M1→N6,7;N6,7)
5 10-4
10-4
(dW/WdE)1/2 in keV-1/2
mν =0
mν =60 eV
Q
2.45
2.50
2.55
2.60
E(keV)

Fig. 25

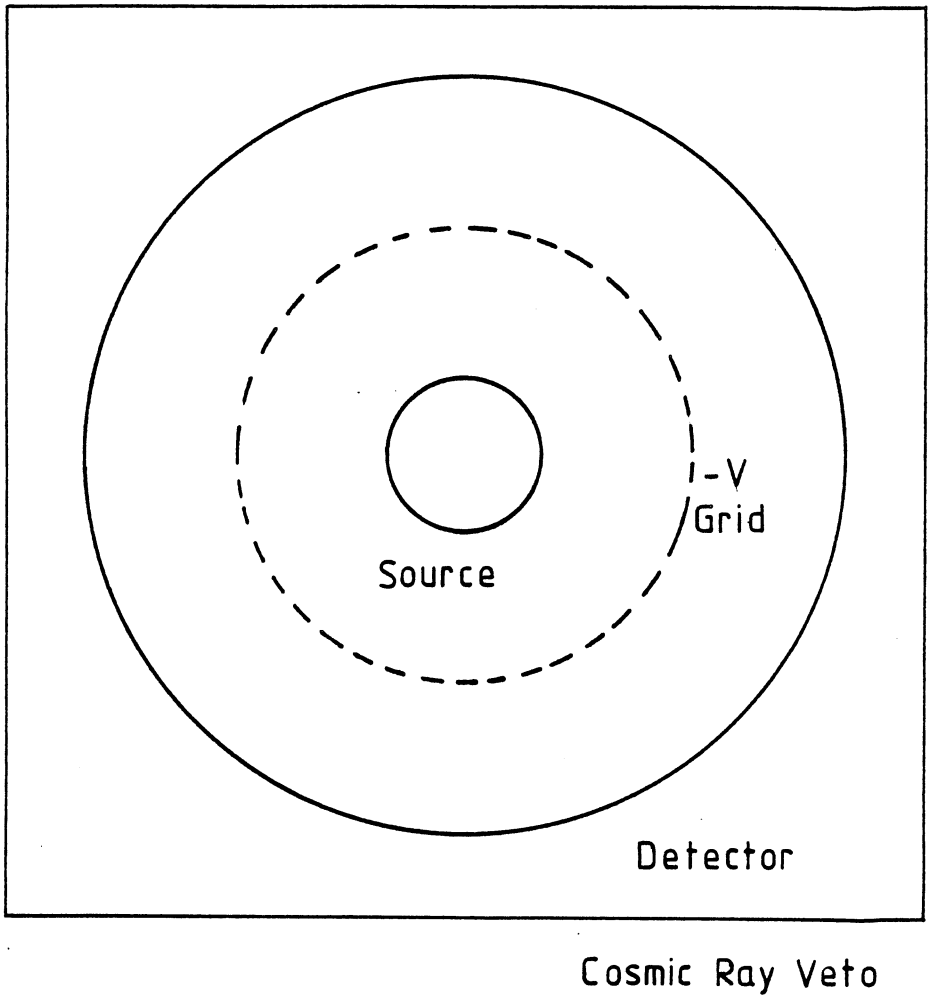

Fig. 26

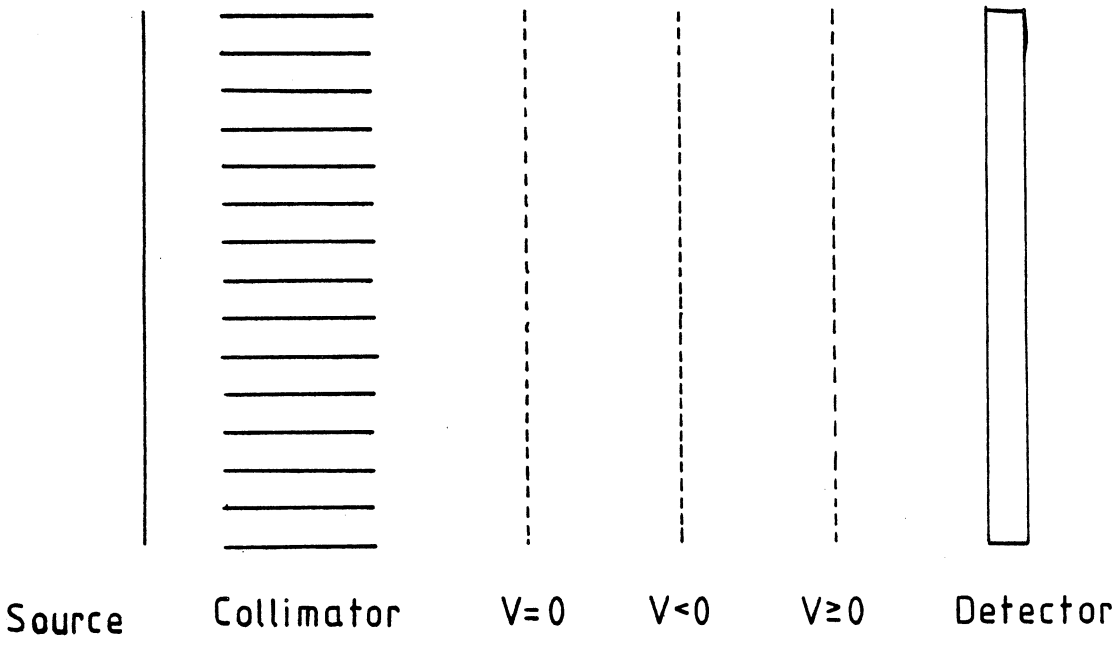

Fig. 27

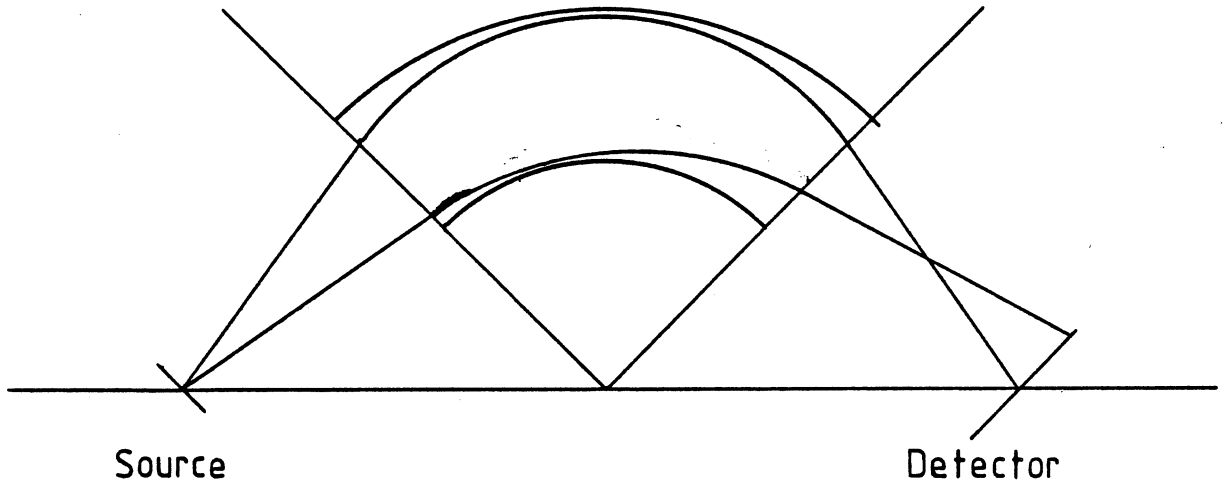

Fig. 28

APPENDIX A

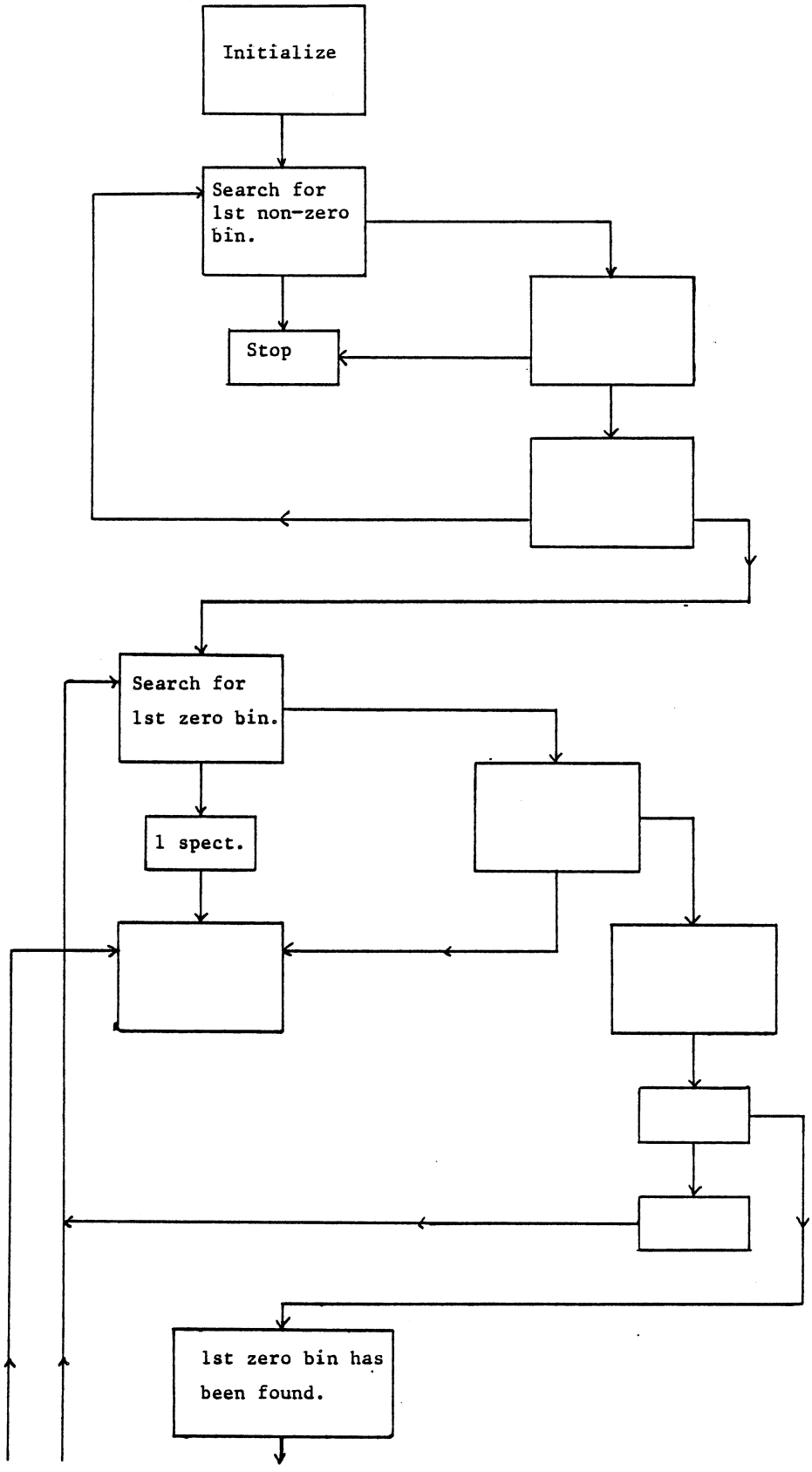
Initialize
Search for 1st non-zero bin.
Stop
Search for 1st zero bin.
1 spect.
1st zero bin has been found.

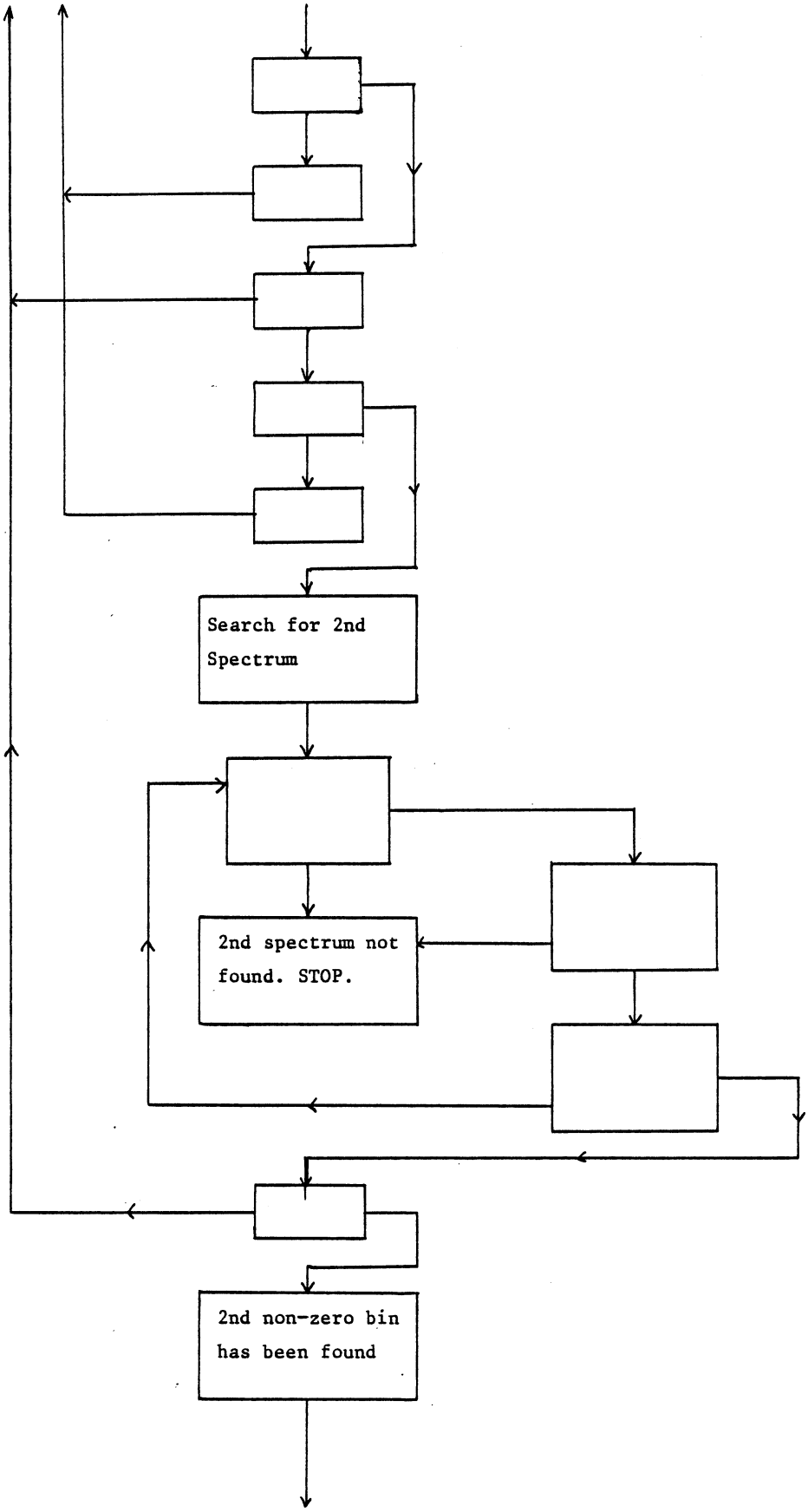
Search for 2nd Spectrum
2nd spectrum not found. STOP.
2nd non-zero bin has been found

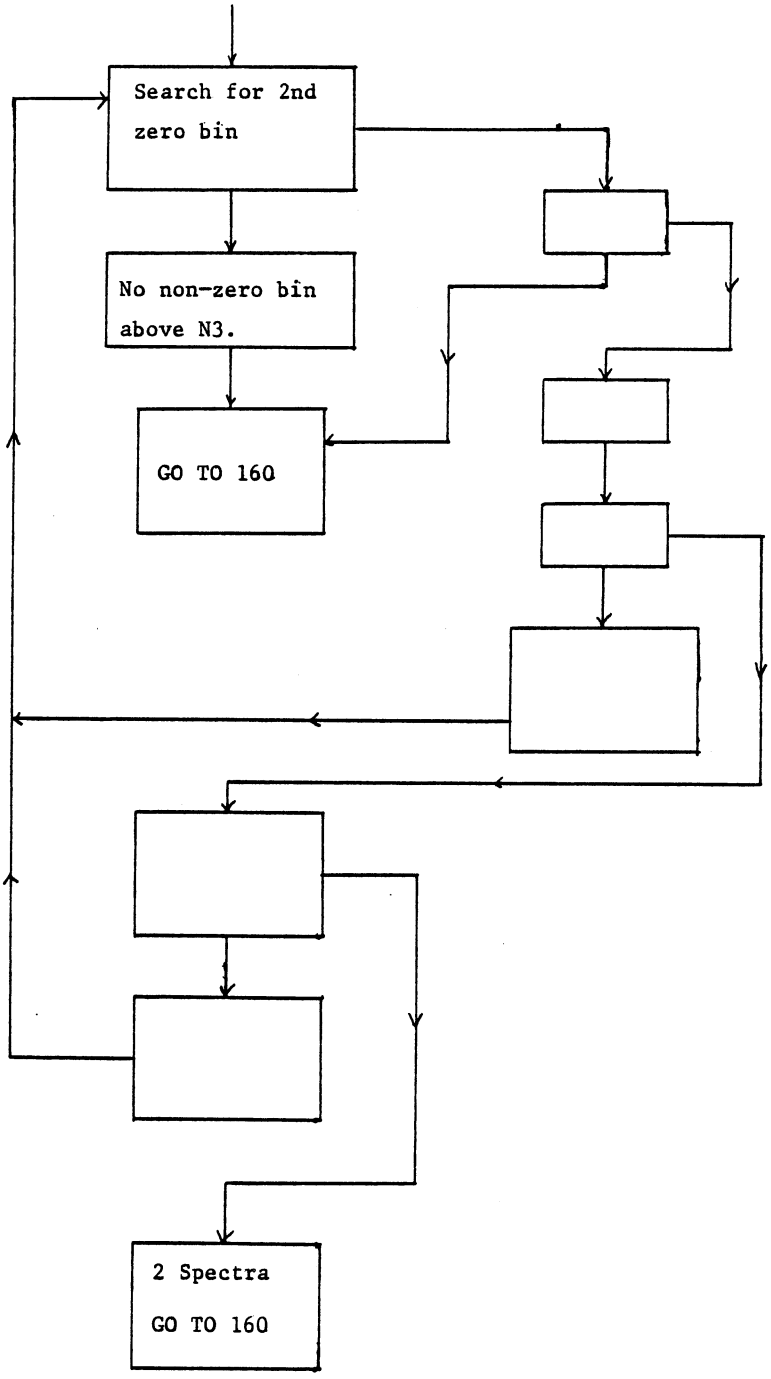
Search for 2nd zero bin
No non-zero bin above N3.
GO TO 160
2 Spectra
GO TO 160

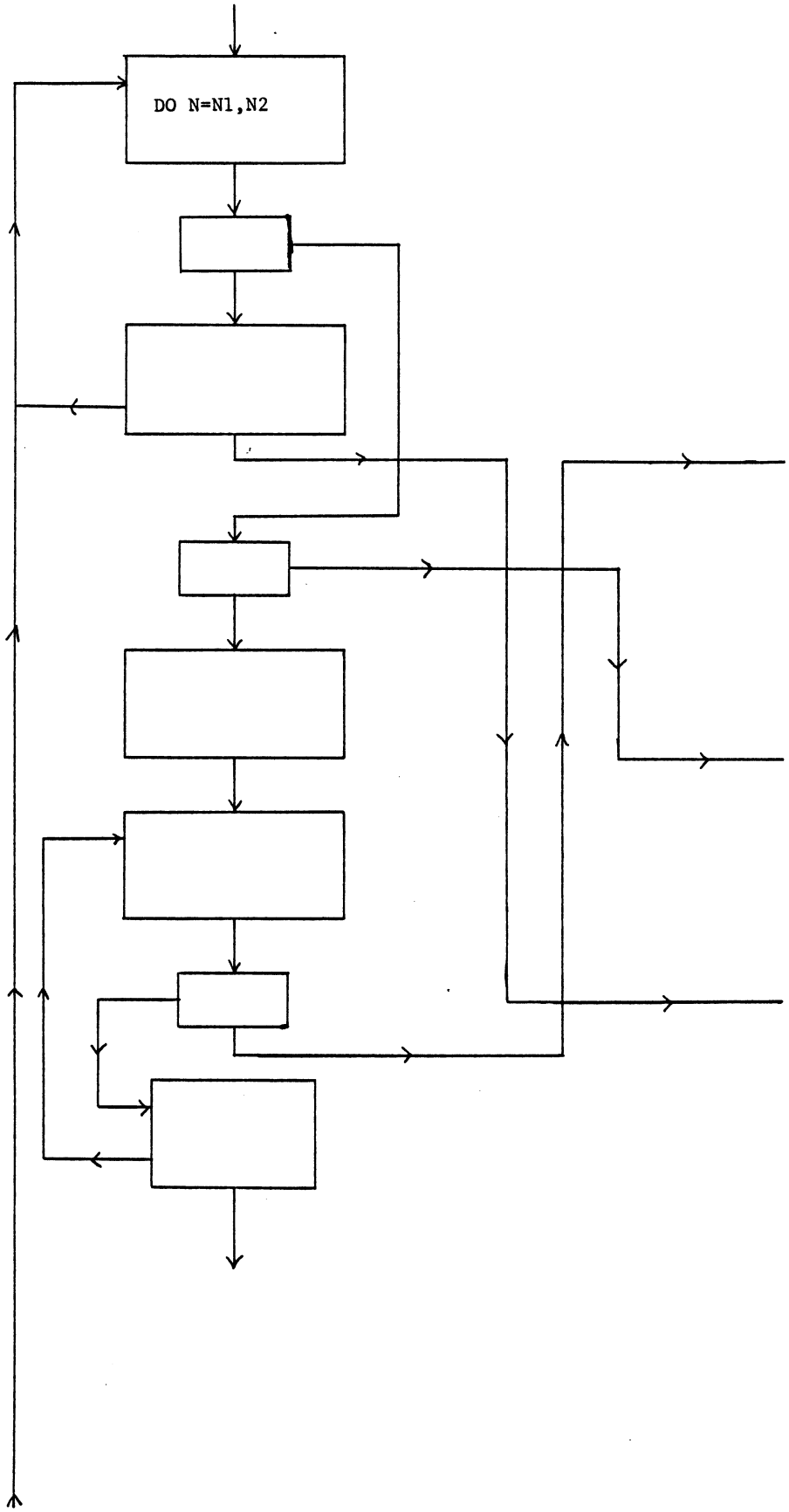
DO N=N1,N2

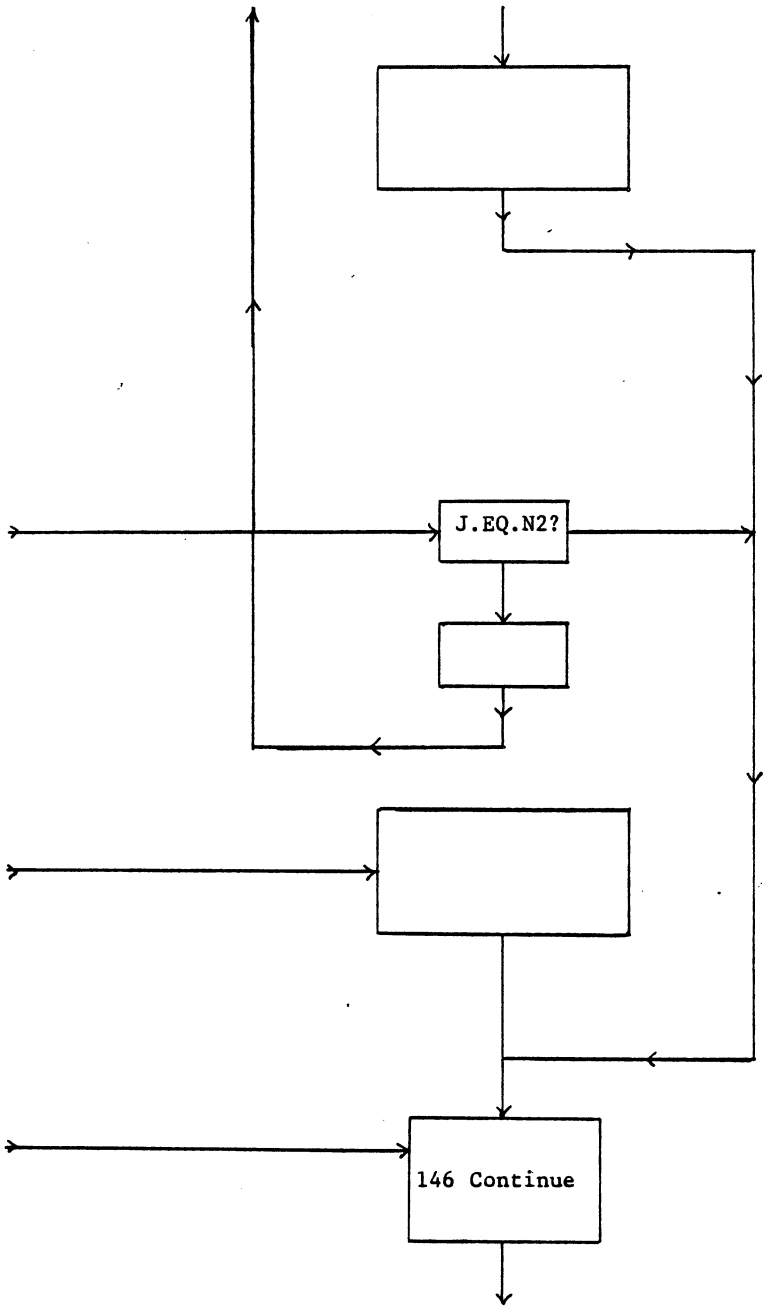
J.EQ.N2?
146 Continue